International Journal of Multiphase Flow 40 (2012) 1–18

Contents lists available at SciVerse ScienceDirect

International Journal of Multiphase Flow

journal homepage: www.elsevier.com/locate/ijmulflow

Review

Analyzing preferential concentration and clustering of inertial particles in turbulence

Romain Monchaux [a], Mickael Bourgoin [b], Alain Cartellier [b,*]

[a] Unité de mécanique, Ecole Nationale Supérieure de Techniques Avancées, ParisTech, Chemin de la Hunière, 91761 Palaiseau Cedex, France
[b] LEGI – Laboratoire des Ecoulements Géophysiques et Industriels, CNRS/UJF/G-INP UMR5519, BP53, 38041 Grenoble, France

ARTICLE INFO

Article history:
Received 9 November 2011
Received in revised form 5 December 2011
Accepted 6 December 2011
Available online 13 December 2011

Keywords:
Preferential concentration
Turbulence
Inertial particles

ABSTRACT

Particle laden flows are of relevant interest in many industrial and natural systems. When the carrier flow is turbulent, a striking feature is the tendency of particles denser than the fluid to inhomogeneously distribute in space, forming clusters and depleted regions. This phenomenon, known as "preferential concentration", has now been extensively investigated since the 1960s. The commonly invoked turbophoretic effect, responsible for the centrifugation of heavy particles outside the turbulent vortices, has recently got more complex by other additional mechanisms which have been shown to potentially play an important role in segregating the particles (for instance particles with moderate Stokes number have been shown to preferentially stick to low-acceleration points of the carrier flow). As a matter of fact a complete frame for accurately describing and modeling the particle-flow interaction is not yet available and basic questions, as the existence or not of a typical cluster size or of a typical cluster life-time-scale, still remain to be answered. This requires further quantitative investigations of preferential concentration (both from experiments and numerics) as well as dedicated mathematical tools in order to analyze the dispersed phase, its structuring properties and its dynamics (from individual particle level up to clusters level). This review focuses on the description of the techniques available nowadays to investigate the preferential concentration of inertial particles in turbulent flows. We first briefly recall the historical context of the problem followed by a description of usual experimental and numerical configurations classically employed to investigate this phenomenon. Then we present the main mathematical analysis techniques which have been developed and implemented up to now to diagnose and characterize the clustering properties of dispersed particles. We show the advantages, drawbacks and complementarity of the different existing approaches. To finish, we present physical mechanisms which have already been identified as important and discuss the expected breakthrough from future investigations.

Contents

* Corresponding author. Tel.: +33 (0)476825048; fax: +33 (0)476825271.
E-mail address: alain.cartellier@legi.grenoble-inp.fr (A. Cartellier).

0301-9322/$ - see front matter © 2011 Elsevier Ltd. All rights reserved.
doi:10.1016/j.ijmultiphaseflow.2011.12.001

1. Introduction

Turbulent flows laden with particles occur very often in natural and industrial situations: dispersion of pollutants in the atmosphere, sedimentation in rivers, rain formation in warm clouds, plankton dispersion in the ocean, optimization of chemical reactors and of various industrial processes including combustion of liquid fuel... In these examples, particles consist of dust/sand in air or water, liquid droplets or solid particles (such as coal, catalyst...) in gas and are then denser than the carrying fluid. Thus, their dynamics is not strictly following the fluid velocity field but is instead lagging behind it. This is a specific case of inertial particles immersed in turbulent flows that also refer to situations when particles are less dense than the fluid or when particles size is much greater than the smallest turbulent scale, namely the Kolmogorov length. The common occurrence of this class of flows deserves thorough fundamental studies since no proper or practical modeling is yet available. So far, the equations governing inertial particle dynamics have been obtained under strong assumptions in very limited situations (Gatignol, 1983; Maxey and Riley, 1983) and most of the recent numerical works use even simpler models.

This review is dedicated to the characterization of the most striking feature in turbulent flows laden with inertial particles: the very strong inhomogeneity of the particle concentration field. Particle Image Velocimetry (PIV) or Laser Doppler Anemometry (LDA) make use of tracer particles whose inertia vanishes and that are expected to exactly follow the fluid velocity field, allowing fluid velocity measurements. If ideal tracer particles are randomly but uniformly distributed in the physical space this is no longer true when particles have some inertia. Fig. 1 presents various snapshots from a numerical simulation of particles in homogeneous and isotropic turbulence (HIT) with increasing inertia. On the first panel, tracers are homogeneously distributed, but as inertia comes into play, strong inhomogeneities appear. This phenomenon is commonly referred to as "preferential concentration" or "clustering", without distinction.

In this review, we would like to explicitly distinguish three aspects of this phenomenon : (i) *preferential concentration*, (ii) *clustering* and (iii) *clusters* as evolutive entities. *Preferential concentration* refers to the fact that particles go preferentially in some particular regions of the flow associated, for example, to some particular values of the strain tensor or of the fluid acceleration: such mechanisms also hold for individual inclusions or in diluted conditions where no accumulation is visually identifiable. We consider *clustering* as the fact that particles tend to accumulate and segregate *i.e.* that both very dense and almost empty regions are created in the flow. Finally we define *clusters* as groups of particles that remain close to one another (and possibly interact) on time scales long compared to some turbulence time scale. *Clustering* then appears as a concentration matter, *preferential concentration* as a selective sampling of the flow and *clusters* as dynamical evolutive entities implying possible collective effects. Regarding the various practical applications and our fundamental understanding of the mechanisms implied in these processes, the three aspects have to be understood. Clustering necessarily implies very high concentration regions which are of prime importance in the cases of pollutant or plankton dispersion, for example, while the existence of clusters is crucial in rain formation or chemical reactions frameworks. Preferential concentration clearly points to the mechanisms responsible for both clustering and cluster evolution.

1.1. Origins and first results regarding preferential concentration

Crowe et al. (1988) trace back to the 1960s early qualitative observations and speculations on the potential role of large eddies on the dispersion of particles. In particular, the existence of significant concentration fluctuations is reported (but not quantified) by Kada and Hanratty (1960) in a turbulent pipe flow laden with heavy spheres. The first indisputable experimental evidence of preferential concentration of dense particles in turbulent flows was obtained for heavy particles interacting with large scale turbulent structures arising in mixing layers, whose existence was identified in 1974 by Brown and Roshko (1974). Among such early contributions, let us quote (Crowe et al., 1985; Chein and Chung, 1988; Tang et al., 1992; Wen et al., 1992; Kobayashi et al., 1992; Lazaro and Lasheras, 1992). Similar behaviors were also reported for jets in the region dominated by vortex ring structures (in particular see Longmire and Eaton, 1992). All these authors observed that particles happen to be scarcely present inside vortices, with the exception of very small Stokes number particles. Instead, and as demonstrated by time resolved analysis of the concentration field, the particles with Stokes numbers close to unity are mostly encountered in the saddle regions between vortex. They are also entrained at the periphery of the large vortices, with strong consequences on their dispersion.

Such features were qualitatively recovered from two-dimensional simulations of particles interacting with large eddies in particular using Stuart vortices (Crowe et al., 1985) or discrete

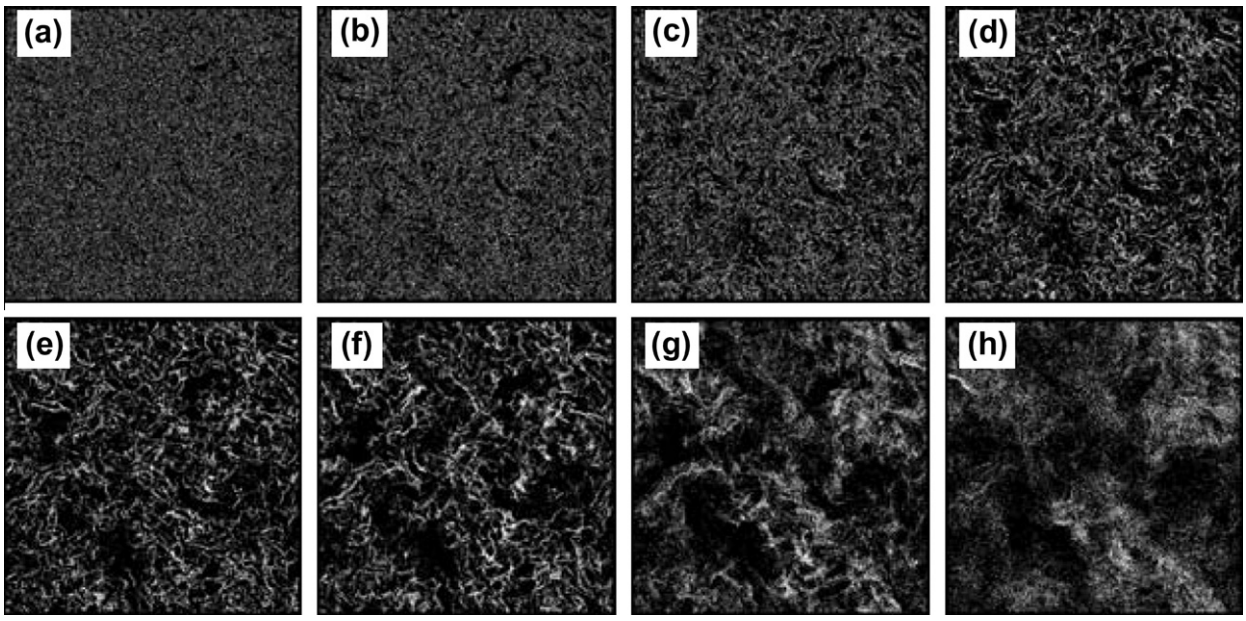

Fig. 1. Spatial distribution of particles inside a thin layer (width $5\eta_K$) for eight different Stokes numbers. The side length of plots is $3.4L \simeq 1100\eta_K$. $t \simeq 2.1T \simeq 100\tau_\eta$. (a) $S_\eta = 0.05$, (b) 0.1, (c) 0.2, (d) 0.5, (e) 1, (f) 2, (g) 5 and (h) 10. Simulation from Yoshimoto and Goto (2007).

vortex methods (Chein and Chung, 1988; Chung and Troutt, 1988). Maxey and Corrsin (1980, 1986) investigated particles interacting with simple cellular flows, and they show that, due to inertia, the Lagrangian statistics following particles can markedly differ from those of fluid elements, that the average settling velocity of particles is altered compared with still conditions and that significant local accumulations do occur.

To better mimic particles interacting with numerous eddies, numerical investigations based on kinematic simulations (KS) have then been undertaken. With KS, Maxey (1987a) identified a clear effect on the settling rate of dense particles depending on their inertia and their fall velocity in still conditions. He showed that the divergence of the particle velocity is positive in regions of high strain rate and low vorticity, which thus correspond to an accumulation of particles: such preferential positions bias the average settling velocity estimate and give rise to an enhanced settling rate compared with the one in still conditions. These early findings prompted more detailed investigations of point particles in HIT using first Direct Numerical Simulations - DNS (see for ex. Squires and Eaton, 1990, 1991; Elghobashi and Truesdell, 1992 for early contributions) and then Large Eddy Simulations – LES (see for ex. Wang and Squires, 1996; Yang and Lei, 1998). Since the early 1990s, the number of experimental, theoretical and simulation based contributions has steadily increased. Investigations mostly focused on the modulation of the turbulence by particles, on particle dispersion, on the clustering and on its consequences on the settling velocity as well as – but to a lesser extent – on the dispersion (see Balachandar and Eaton, 2010 for a recent review). In the following, we will concentrate on HIT situations but a variety of flow conditions have also been considered including turbulent shear flows (for ex. Ahmed and Elghobashi, 2001; Gualtieri et al., 2009), boundary layer flows with important issues related with particle deposition/resuspension process (for ex. Soldati and Marchioli, 2009; Vinkovic et al., 2011). Investigations have also been extended to very dense systems where collisions (Zaichik et al., 2010) and coalescence (Siebert et al., 2010) need to be accounted for, to non spherical inclusions including agglomerates (see for example Dietzel and Sommerfeld, 2010; Hoelzer and Sommerfeld, 2006), charged particles (for ex. Lu et al., 2010)... not to forget the current progress dedicated to account for the finite size of particles (which will be evoked later in the text).

In all these approaches, there is a need for demonstrating the existence of preferential concentration, for quantifying it, and also for relating its features to specific characteristics of the continuous phase. In the following, we review and compare a number of methods which have been developed to accomplish these tasks on data sets arising from simulations as well as from experiments.

If most of the pioneering studies concern structured flows (shear layers, boundary layers, free jets, wakes...), this review focuses on homogeneous and isotropic turbulence (HIT) which is a usual paradigm, numerically as well as experimentally. Section 2 summarizes experimental and numerical configurations currently used to study inertial particle-laden flows and insists on the main limitations and difficulties encountered in both cases, Section 3 presents and compares the various indicators and post-processing methods developed to characterize, quantify and analyze preferential concentration and clustering. In Section 4 we discuss several physical mechanisms relevant in the context of the preferential concentration phenomenon. We conclude this article with some expected future breakthrough on experimental, numerical and conceptual grounds (Section 5).

2. Experimental and numerical configuration

Up to the eighties, most of the work was performed experimentally but, in this field, numerical simulations share has drastically increased in the last thirty years while the experimental effort was somewhat shrinking. References in the present review are then mostly related to numerical works, even if we have tried to collect as many experimental contributions as possible.

2.1. Experimental facilities

As mentioned in the introduction, recent research is mostly focused on homogeneous and isotropic turbulence (HIT) rather than on structured flows, with the exception of boundary layer flows which are receiving a renewed attention. Preferential

concentration has been widely studied in a variety of anisotropic flows including free shear flows, mixing layers, boundary layers, turbulent jets, bluff body... and for these we refer the reader to the review by Eaton and Fessler (1994). We describe hereafter the two, more or less, classical ways to approach HIT.

2.1.1. Wind-tunnel experiments

These flows are produced with fans blowing into a large-section tunnel. Turbulence is generated behind a grid that is placed downstream a convergent section that accelerates the fluid in order to reach moderate Reynolds numbers. Since these flows have been widely used since the sixties to investigate turbulence statistical properties, a large literature is available on the optimal designs of the grids in terms of mesh size and solidity. These parameters control the integral scale as well as the Taylor micro-scale based Reynolds number value (R_λ, referred to as Reynolds number in the following). Sizes of wind tunnels are broadly distributed, with test sections ranging from 10 to 100 cm for typical laboratory experiments and up to several meters for the largest apparatuses like the one in Modane–Avrieux which has a test section 8 m wide and 14 m long. Consequently, reachable Reynolds numbers are also spanning a wide range, from 100 to 400 in classical tunnels to several thousands in very large experimental facilities. Bodenschatz team in Goettingen is currently operating a classical wind tunnel filled with SF_6 gas the very low viscosity of which allows them to reach higher Reynolds numbers exceeding a few thousands (Bodenschatz, 2009). More recently, different teams have introduced active grids that allow much higher R_λ values in "small" laboratory experiments (see Saw et al., 2008 for example). The active-grid technology is tricky since these grids consist of rotating panels more or less independent so that several classical parameters as solidity or mesh size are not constant during the experiment and the impact on the generated turbulence of the way these panels are moved is not always easy to quantify.

If wind-tunnel turbulence produces well controlled flows, the main difficulty resides in the seeding. Solid particles can be used in open tunnels. They are avoided in closed loops because of the required separation technique, of the fragility of fans... Water droplets generated by different types of commercial injectors are used instead. When using injectors, the control of the particle size polydispersity is often an issue. The other common difficulty concerns the spatial homogeneity of the seeding. Experiments used in the context of the present article are operated in Grenoble (Monchaux et al., 2010), in Cornell (Ayyalasomayajula et al., 2006) and in San Diego (Aliseda et al., 2002).

2.1.2. Closed flows

In closed flows, seeding is not any more a problem since it is actually easy to use calibrated beads of various densities that remain in the vessel and do not interfere with the propellers. The only problems arise with particles of very high densities compared to the carrier flow that tend to settle very fast with respect to the experiment duration. We present two families of closed flows used to study preferential concentration.

Von Kármán experiments consist of counter rotating propellers usually embedded in a closed vessel. Forcing efficiency is good enough to reach very high Reynolds numbers (typically $R_\lambda \simeq 400$ or more) with relatively low power injected. The resulting flow is strongly inhomogeneous and anisotropic. Nevertheless, many teams have worked around the central stagnation point where the mean flow is weak so that at least homogeneity is almost recovered.

Different extensions of the von Kármán facilities have been designed. They consist of many (at least 8) motors randomly rotating on the faces of a polyhedral volume. A cubic box fitted with eight fans is operated in Buffalo (Salazar et al., 2008) while similar turbulence boxes in icosahedron geometry are currently developed by at least two teams in ENS Lyon and at the Max Planck Institute in Goettingen (Zimmermann et al., 2010; Gibert et al., 2010) in order to get more homogeneous and isotropic flows. All these experiments inherit the von Kármán setup advantages and drawbacks but achieve almost HIT flows. An alternative strategy has been proposed by Hwang and Eaton (2004) and followed recently in LMFA Lyon (Goepfert et al., 2010) to generate isotropic turbulence in air using synthetic jets. Turbulent boxes have also been exploited by other teams (see Fallon and Rogers, 2002; Friedman and Katz, 2002; Guala et al., 2008; Yang and Shy, 2005).

2.2. Numerical approaches

As already mentioned, in the late years, the number of numerical simulations dedicated to particle-laden flows has been flourishing. We can distinguish three classes of simulations: direct numerical simulations (DNS) or large eddy simulations (LES) of the Navier–Stokes equations, random flows and synthetic flows. The latter two aim at capturing specific features of the natural processes while the former try to be close to the actual phenomenon even if the forces actually acting on the particles, generally assumed to be point particles, are not properly modeled so far.

2.2.1. Direct numerical simulations and large eddies simulations

To date, the almost simultaneous works by Maxey and Riley (1983) and Gatignol (1983) in 1983 are the best evaluations of the forces acting on a point particle in a turbulent flow and all the numerical studies dealing with point particles have almost systematically relied on them until recently. Almost all of them consider point particles whose density is much higher than that of the fluid so that the only remaining force acting on the particles is the drag force, the latter being usually evaluated as a Stokes drag. The resulting dynamical equation is:

$$\frac{\partial \mathbf{v}_p}{\partial t} = -\frac{1}{\tau_p}(\mathbf{v}_p(t) - \mathbf{u}(\mathbf{x}_p, t)), \tag{1}$$

where $\mathbf{x}_p$ and $\mathbf{v}_p$ are the particle position and velocity, $\mathbf{u}$ is the fluid velocity and τ_p is the viscous response time of the particle, also called Stokes time scale. Expression (1) corresponds to neglecting gravity, and assuming that the particle radii r are much smaller than the Kolmogorov length η_K, that the relative velocity between the particles and the surrounding fluid and r are such that the corresponding Reynolds number is compatible with the Stokes approximation and that the particle density is much higher than that of the fluid. Usually, the Navier–Stokes equations are solved in a square or cubic box – whose size depends on the resolution of the simulation – to obtain $\mathbf{u}$. This fluid velocity field is then used to solve Eq. (1). This method (referred in the present as one-way simulations) is then compatible with the dilute limits that exclude the possibility of two-way coupling (see Section 2.3). To our knowledge, only Elghobashi and Truesdell (1992), Ferrante and Elghobashi (2003) have attempted to model all the forces acting on the particles derived by Maxey and Riley, they solve simultaneously the equations for the fluid and for the particles in presence of gravity for a mass loading ratio of 1. Recently, Faxen corrections (Gatignol (1983)) have been taken into account in one-way simulations in an attempt to simulate finite size effects (Calzavarini et al. (2009)). New approaches resolving the particle finite size are now emerging which offer a very promising perspective to capture subtle inertial effects, either for isolated inclusions see Burton and Eaton (2005), Homann and Bec (2010), Naso and Prosperetti (2010), and Zeng et al. (2010) as well as on many freely moving particles (see Zhang et al., 2006; Uhlmann, 2008; Yeo et al., 2010; Lucci et al., 2010, 2011). Recent contributions from Elghobashi's group are particularly interesting

in the context of the present review as they address the question of preferential concentration of finite size particles and its consequences on turbulence modulation.

2.2.2. Random flows

Initially developed to study statistical properties of turbulence, random flows and more particularly Kraichnan's flows (Kraichnan, 1968) are playing an important role in our understanding of particle-laden flows. Flows belonging to the so-called Kraichnan ensemble consist of delta-correlated in time and spatially correlated flows for which the second order structure function can be written as:

$$\langle \hat{u}_i(r,t)\hat{u}_j(r',t')\rangle = 2b^{ij}(r-r')\delta(t-t'), \tag{2}$$

where $\hat{u}$ is the velocity difference vector field. The spatial correlation tensor b^{ij} is chosen to ensure incompressibility, isotropy and scale invariance. Its expression involve the Hölder exponent h. Playing with h values allows to mimic smooth differentiable velocity fields ($h = 1$ equivalent to dissipative range of turbulence) or rougher flows ($h < 1$ equivalent to inertial range of turbulence). In this framework, the particle dynamics is a Markov process and pair separation for example can be described with a Fokker–Planck equation with multiplicative noise. Bec and co-workers used a model reduction in which the noise becomes additive but at the cost of an additional non-linear drift (see the short review by Bec et al., 2008). Without temporal correlation, these models cannot represent persistent structures, Olla has recently weakened the delta-correlation in time hypothesis to allow some memory effect in the dynamics (Olla, 2010).

2.2.3. Synthetic flows

An important class of flows used to test various ideas and isolate physical mechanisms is the so-called synthetic flows or kinematic simulations. The latter consist of a superimposition of sine and cosine functions that mimic turbulent behavior as for example:

$$\mathbf{u}(\mathbf{x},t) = \sum_{n=1}^{N_k} \mathbf{A}_n \sin(\mathbf{k}_n\cdot\mathbf{x}+\omega_n t) + \mathbf{B}_n \cos(\mathbf{k}_n\cdot\mathbf{x}+\omega_n t), \tag{3}$$

$\mathbf{A}_n$ and $\mathbf{B}_n$ are chosen to establish a prescribed energy spectrum and are normal to $\mathbf{k}_n$ to ensure incompressibility. This type of model has been used by various authors Chen et al. (2006) and Ijzermans et al. (2010) in the framework of inertial particle preferential concentration in comparison to more realistic approaches.

Synthetic flows would refer to flows built with arrays of analytical vortices whose relative positions or intensity are randomly or deterministically evolving or built from superimposition of various pure shear flows whose intensity is also randomly evolving. These minimal models have been used for long to test basic vortex trapping/escaping ideas by Eaton and Fessler (1994) or Maxey (1987b) but in a more recent literature as well (Bec et al., 2005; Ijzermans et al., 2010; Ducasse and Pumir, 2009; Aly and Nicolleau, 2008).

2.3. Seeding techniques and particle characterization

An obviously crucial point in the preferential concentration studies is the seeding and, according to the particles employed, their characterization. There are different aspects to take into account when dealing with seeding: some concern the particle characteristics as their size, density or shape while others concern the particle field as the mass or volume fraction loading, the loading homogeneity or the relative seeding injection velocity. At this stage, it is important to define and discuss the control parameters associated to particle-laden turbulent flows. The most relevant control parameters governing turbulent flows laden with inertial particles are the Stokes and Rouse numbers and the mass and volume loading. The Stokes number compares the particle viscous relaxation time to a turbulent time. The latter is often chosen as the Kolmogorov time, but can also be chosen somewhere else in the inertial range or in the large scales. The Rouse number compares the particle terminal velocity to the turbulent fluctuations intensity. In dispersed systems, the loading intervenes both by way of the volume concentration and by way of the mass loading. The latter is known to have a significant effect on the turbulence modulation (Druzhinin and Elghobashi, 1999) while the volume concentration primarily affects the momentum coupling between phases.

2.3.1. Particle seeding

Intuitively, mass and volume fraction loading should only impact the coupling between the fluid and the dispersed phases, nevertheless, different studies have pointed out some possible collective dynamics leading to non trivial effects of global concentration on settling velocity of the particles or on the clustering properties (see for example Aliseda et al., 2002 or Monchaux et al., 2010). Even if a clear threshold cannot be defined, it is generally assumed that for volume fraction (*resp.* mass loading) less than 10^{-5} (*resp.* 10^{-2}) the fluid flow is not affected by the particles that may be considered as passively advected. Above these values, back reaction of the particles on the fluid cannot be ruled out anymore. In addition, collisions are to be accounted for volume fractions exceeding typically 10^{-3}. Note that investigations of the so-called two-way coupling problem are still scarce (see Ferrante and Elghobashi, 2003; Lucci et al., 2010, 2011 for the most extensive numerical studies) and much remains to be understood on the influence of the loading. Moreover, the crude estimates given above are expected to evolve when taking into account the finite size of particles as notably shown by Yeo et al. (2010) and by Lucci et al. (2010, 2011). Let us finally mention that new parameters have been recently proposed to account for the modulation of turbulence. For instance, Poelma et al. (2007) proposed to use a "Stokes load" defined as $\Phi_{St} = n'St$ (with St the usual Stokes number and n' the average number of particles in a dissipative eddy) which they have shown to give a better collapse of experimental data on turbulence modulation (see also the reviews by Poelma and Ooms, 2006; Balachandar and Eaton, 2010 on this question).

In almost any numerical study, particles are injected in the simulation at once at uniformly distributed random locations covering the whole computation box, which seems to be the ideal way to inject particles if one wants to study the segregation and preferential concentration occurring to the particle field. Experimentally people try to adopt seeding techniques leading to situations as close as possible to the ideal numerical case. In closed flows and turbulent boxes seeded with particles whose density is not very different from the fluid's one the seeding homogeneity is not a problem. Difficulties arise for particles much denser than the fluid that tend to settle quickly – even in von Kármaán flows that are very efficient mixing flows – and basically, this phenomenon drastically limits the experiment duration and implies some pre-mixing before each experiment. Wind tunnel experiment is probably the most challenging situation since the settling problem (that may also induce some secondary flow in the carrier phase) is complemented with the injection uniformity issue. Usually, particles are injected far enough upstream the measurement volume, typically close to the grid location. The injection process should avoid creating disturbances to the flow (wakes, mixing layers...) and should achieve homogeneous seeding. The solution chosen often implies an array of injectors placed on the grid itself and aiming at the downstream direction, or surrounding the grid and aiming at the center of the tunnel.

The initial velocity difference between particles and carrier fluid implies the possible formation of mixing layers that would result in persistent structures developing along the flow.

2.3.2. Particle characterization

Regarding the particle characteristics, the most comfortable situation occurs when only one type of particle is present so that results are easier to analyze since the Stokes number for example is non ambiguously defined. If monodispersity is easily approached in the case of solid particles that can be calibrated, seeding with droplets leads to strongly polydispersed particle populations. A careful characterization of the particle properties is then required to evaluate the size distribution. Aside direct imaging techniques, several systems exist to achieve in situ measurements such as Phase Doppler Anemometers (PDAs, commercialized for instance by Artium Technologies, TSI, Dantec Dynamics), diffraction based analyzers – such as the SprayTech by Malvern (UK) –, phase detection optical probes – see for instance A2 Photonic Sensors (France)…, interferometric particle imaging and global phase Doppler techniques, see for example Damaschke et al. (2002)… Except in the case of PDA and phase detection probes (see Hong et al., 2004; Saito et al., 2009), the granulometry analysis has to be performed independently from velocity or concentration measurements (to be described in the next section). If we implicitly assume here that particles are spherical and are thus fully characterized by their diameter, some experiments have been operated with more complicated particles such as pollen or with living organisms with or without mobility whose shape is far from spherical (see for instance Schmitt and Seuront (2008)).

2.3.3. Stokes number

Among the key parameters governing turbulent flows laden with dense particles, the Stokes number defined as the particle response time relative to some time scale characteristics of the underlying continuous phase flow (generally the Kolmogorov time scale τ_η or the integral time scale of the carrier flow $T = L/u'$, where L is the correlation length of the carrier velocity field and u' its *rms* value) plays a central role. Its definition and evaluation thus deserve a careful examination. The classical definition compares the viscous relaxation time of the particle τ_v and the Kolmogorov time τ_η:

$$St = \frac{\tau_v}{\tau_\eta} \quad \text{with } \tau_v = \frac{1}{18}\frac{\rho_p}{\rho_f}\frac{d_p^2}{\nu}, \tag{4}$$

where ρ_p and ρ_f are the particle and fluid density, ν is the fluid kinematic viscosity and d_p is the particle diameter.

Although this Stokes number is commonly said to represent inertial effects, recent investigations of the dynamics of isolated inclusions (Qureshi et al., 2007, 2008) indicate that – for a given Stokes number – size and density are not interchangeable quantities in terms of particle dynamics, and therefore they ought to be distinguished in future investigations dealing with finite size inclusions. Recent two-way coupling simulations by Lucci et al. (2010, 2011) are considering particles whose diameters are around the Taylor micro-scale. They do show that particles with same relaxation time but with different diameters have different impact on the carrier flow. Thus, the relevant parameter space is at least two dimensional. To account for the particle finite sizes one cannot use τ_v nor τ_η anymore and we refer the reader to a recent discussion of this point by Xu and Bodenschatz (2008) and by Schmitt and Seuront (2008). Both teams consider that the particles filter the turbulent motion happening at scales smaller than their diameter and use the turbulent dynamical time at the scale of the particle size:

$$\tau_p = \left(\frac{d_p^2}{\epsilon}\right)^{1/3}, \tag{5}$$

leading to Stokes number values smaller than those defined from the Kolmogorov time scale. Similarly, even when the point particle approximation is valid, following an original idea by Falkovich et al. (2003) and Bec et al. (2007b, 2008) have shown that scale by scale clustering properties in the inertial range may be better described in terms of a local Stokes number, defined as the ratio between the particle response time τ_v and the turnover time at the given scale of interest. Further corrections are also to be considered if the particulate Reynolds number increases, thus either for large particles or for particles with large relative velocity with respect to the fluid (see for instance Mei, 1996).

From an experimental point of view, evaluation of the Stokes number is most of the time a tricky problem. In the case of polydispersed seedings, if one wants to define a Stokes number associated to one experiment, the particle diameter used in the Stokes number calculation is a statistical quantity (mean or more probable value for example) whose dispersion (measured with the variance of the particle diameters distribution) could be large compared to the mean. Other complications arise from the turbulent times definitions that require the measurement of the dissipation rate ϵ which is also often subject to large uncertainties. As a result, it is often delicate to compare exact absolute Stokes numbers values obtained from different experiments for which size distributions are most often polydispersed.

3. Diagnosis for preferential concentration and clusters characterization

In this section, we will describe the many methods used to study and characterize preferential concentration and clustering in turbulent flows. First, we focus on direct methods that are all more or less linked to concentration measurements. Then we present some indirect methods that use dynamical measurements to evidence a preferential sampling of the flow by inertial particles. We close this section by mentioning the few attempts to perform simultaneous measurements in the continuous and dispersed phases.

Ideally, one aims at knowing exact 3D coordinates of all the particles present in the flow but practically we are still lagging very far behind this goal. Several teams have developed sophisticated 3D particle tracking (Ayyalasomayajula et al., 2006; Luthi, 2003) that allows to follow several hundreds of particle trajectories in a small volume (whose typical size is of the order of $4-5$ cm) at a quite high cost since it requires the use of four high speed cameras and implies the use of a cluster to process the acquired images in a reasonable amount of time. For the matter of preferential concentration, these data can be very useful for indirect dynamical methods but are not very suited to the study of concentration fields since the number of particles tracked per unit volume is limited. 3*D* data may also come from holographic methods as developed for example at Buffalo or Lyon (Chareyron, 2009; Salazar et al., 2008), even if to date, the number of particles followed with this technique is still low ($\simeq$400 typically). The most common acquisition consists of 2D-pictures taken in a thin laser sheet (usually of the order of 1 mm). The great advantage is that these pictures contain many particles (from 1000 to 20,000 typically) distributed on lengths comparable with the flow integral scale, allowing good concentration measurement and cluster characterization. Flows being necessarily 3D, using 2D-pictures implies a projection of the particle positions over the laser sheet thickness (the resulting bias has to be carefully evaluated) and, according to the flow topology, makes particle tracking noisy to perform (quasi 2D flows as

wind-tunnel) or impossible (fully 3D flows as von Kármán flows). Finally, we note that, in some situations, people use 1D data consisting of single point measurement of particle arrival time (typically from PDA or from in situ measurements in clouds). From those, using a kind of Taylor hypothesis, they build a 1D concentration map along a line. Numerical simulations may also be 1D, 2D or 3D and in the following paragraph, we will describe the type of analysis that can be performed from such data to get insight into the preferential concentration and clustering issues.

3.1. Quantifying preferential concentration/clustering

If visualizations give qualitative impressions of the strength of the preferential concentration phenomenon, there is a tremendous call for quantitative estimations of it and several approaches are simultaneously used to achieve this goal. In the introduction, we defined what we mean by *preferential concentration*, *clustering* and *clusters*; in this section we review several methods which are used to analyze particles in turbulent flows and we discuss to which extent they allow, or not, to characterize these three phenomena. In order to compare these different analysis techniques, whenever it was possible, we have processed data acquired in our wind-tunnel and described in Monchaux et al. (2010) with each method.

3.1.1. A wide range of methods

When dealing with preferential concentration or clustering, it is implicitly assumed that one deals with preferential concentration when compared to uniformly distributed particles leading to a Poisson distribution. Almost all the hereafter described methods try to quantify a distance between the considered concentration fields and uniform ones.

3.1.1.1. Visualizations. Qualitative analysis of clustering and preferential concentration is often given through visualizations, particularly in numerical papers. Whatever are the simulations, 2D DNS (Chen et al., 2006; Goto and Vassilicos, 2006; Coleman and Vassilicos, 2009), 3D DNS (Squires and Eaton, 1990, 1991; Wang and Maxey, 1993; Reade and Collins, 2000; Collins and Keswani, 2004; Bec et al., 2007a; Calzavarini et al., 2008; Goto and Vassilicos, 2008; Coleman and Vassilicos, 2009; Bec et al., 2010; Yoshimoto and Goto, 2007), Large Eddy Simulations, Wang and Squires (1996) and Jin et al. (2010) stochastic modeling (Bec, 2005; Bec et al., 2005) authors often display series of pictures associated to Stokes numbers increasing from the tracer limit up to order 10 values as shown in Fig. 1 taken from Yoshimoto and Goto (2007). Results are actually consistent among these various publications, even if the forces acting on particles are differently modeled: for tracers, the particles are homogeneously distributed and as Stokes number is increasing some areas get denser and denser while others are drained; maximum concentration gradients are observed for Stokes numbers around unity above which empty areas stop growing while concentration patterns in dense area turn blurred. Visualizations have been also used to point out correlations between particle concentration and either region of high/low strain or fluid zero-acceleration points (Chen et al., 2006; Coleman and Vassilicos, 2009; Goto and Vassilicos, 2006; Goto and Vassilicos, 2008) or pressure gradient fields (Bec et al., 2007a). We will see later how quantitative indicators support these visualizations. Experimentally, this type of visualizations is scarcely used in a direct way but, as already mentioned, preferential concentration is often employed for flow visualization purposes. We also remark that the review by Eaton and Fessler (1994) refers to a large number of visualizations in complex and structured flows.

3.1.1.2. Clustering index. This is a rough way to obtain something close to the box index described below. A test volume V is chosen and moved in the whole space. For each position of the test volume, N is the number of particles within in the volume at the considered position. One defines the clustering index (CI) as:

$$CI(V) = \frac{\sigma_N}{\overline{N}} - 1, \tag{6}$$

where $\overline{N}$ and σ_N are the average and the variance of the numbers of particles $N(V)$ obtained when moving the test volume. For Poisson distributions, as mean and variance are equal, CI is identically equal to zero while it gets positive when spatial correlations occur in V. The review by Shaw et al. (2002) references teams that used the clustering index to quantify clustering in clouds. The clustering index strongly depends on the scale chosen to define the control volume V and is thus scarcely used.

3.1.1.3. Box counting methods. Starting from nD-data, whatever the integer value of n, the nD space is divided into N boxes of equal size defined by an arbitrary chosen scale r such that each box has a volume r^n and that the N boxes fill the entire space of the data. If one wants to measure concentration and/or characterize dense area, then one counts how many particles belong to each box. In the case of uniformly distributed particles, the Probability Density Function (PDF) of the number of particles per box is described by a Poisson distribution. In presence of clustering, boxes with very high and very low number of particles per box will be much more likely to exist than in the Poisson case and so the associated PDF will differ from the associated Poisson one as can be seen from Fig. 2 left obtained with experimental data in presence of clustering. It is then possible to calculate the distance between these two PDF with

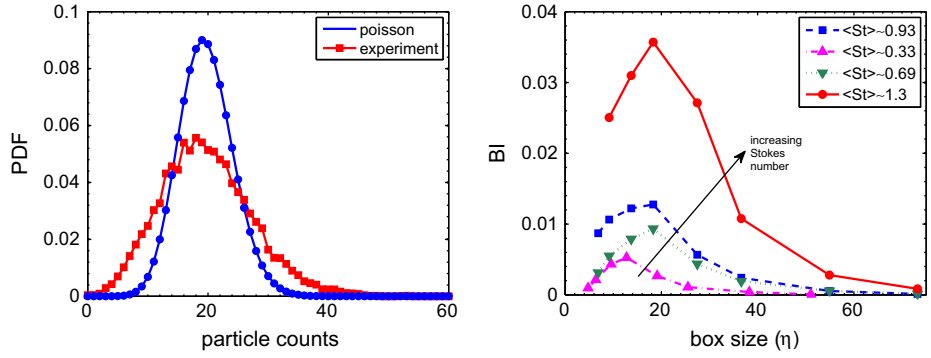

Fig. 2. Box counting method. Left: PDF of the number of particles per box for an experiment (red squares) and for an associated Poisson process (blue circles). Right: box index dependence with box sizes for different experiments at various Stokes numbers. The average number of particles per image varies in the range 600–4000. Experiments taken from Monchaux et al. (2010). (For interpretation of the references to color in this figure legend, the reader is referred to the web version of this article.)

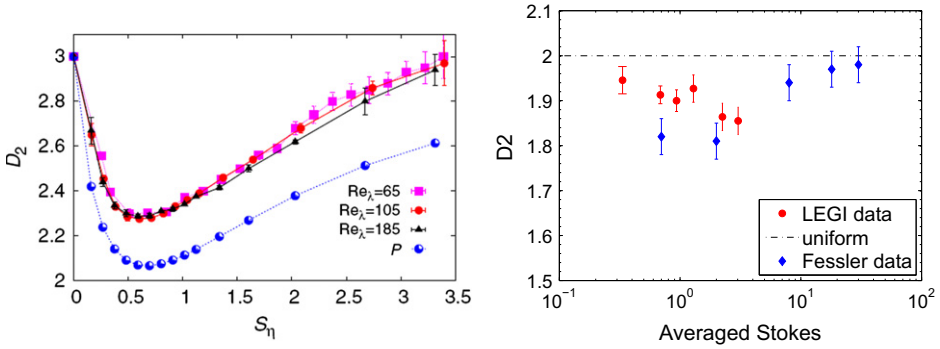

Fig. 3. The correlation dimension D_2 vs S_η. Left: for the three different Re_λ in simulations from Bec et al. (2007a), also shown the probability P to find particles in non-hyperbolic (rotating) regions of the flow, for Re_λ = 185 (multiplied by an arbitrary factor for plotting purposes). Right: from experimental data by Fessler et al. (1994) and from experiments at LEGI by Monchaux et al. (2010).

some appropriate norm to obtain a single scalar that characterizes how far the particle distribution is from a uniform one. We will refer to this scalar as box index (*BI*). In this method, the scale r can be arbitrarily chosen at the processing level. On the one hand, this is unsatisfactory since it introduces extrinsically a scale in the processing but on the other hand, if one repeats the processing for various values of the box size r, one may study the particle clustering scale by scale. In Lasheras team (Aliseda et al. (2002)), this has been employed to point out that clustering effect is maximum at scales of order $10\eta_K$. The same analysis performed on data set gathered in the experiment by Monchaux et al. (2010) are presented on the right panel of Fig. 2. The dependence of the Box Index with the box size is shown for different experiments. All curves have the same shape and whatever the value of the Stokes number, the BI is maximum for box sizes of order $10\eta_K$. One notices that the curves associated to Stokes numbers closer to 1 are shifted upward, evidencing the enhancement of preferential concentration in that case.

3.1.1.4. Correlation dimension. This quantity has been introduced in the field of preferential concentration by Tang et al. (1992) and then used by many teams (Fessler et al., 1994; Hogan and Cuzzi, 2001; Bec et al., 2007a). It comes from dissipative dynamical system theory (see references in Bec et al., 2008) and is defined as the exponent of the power-law behavior at small scales of the probability $P_2(r)$ to find two particles at a distance less or equal to r:

$$D_2(r) = \lim_{r\to 0} d_2(R); \quad d_2(r) = \frac{d\ln P_2(r)}{d\ln r}. \tag{7}$$

When particles are uniformly distributed, D_2 is equal to the space dimension, but when the particles cluster (on a fractal set), D_2 decreases. The correlation dimension D_2 is also a simple scalar quantity quantifying the distance to the random uniform distribution. Fig. 3 shows the dependence of D_2 with the Stokes number in a THI numerical simulation, in a turbulent water channel flow from Fessler et al. (1994) and in a wind tunnel from Monchaux et al. (2010). For the three situations, the correlation dimension presents a minimum for Stokes numbers around unity. The three minimum do not exactly happen for the same value of the Stokes number which can be linked to the difficulties existing in defining/measuring the Stokes number (see Section 2.3).

3.1.1.5. Pair correlation. This indicator is clearly the most widely used in the literature. Considering two elementary volumes (dV_1 and dV_2) situated at a distance r away of each other, the probability to find one particle in each of these volumes is given by:

$$P_r(1,2) = (\bar{n}dV_1)(\bar{n}dV_2)\eta(r), \tag{8}$$

$\bar{n}$ being the mean droplet number density. If the concentration is uniformly distributed without any spatial correlations, then $\eta(r)$ is identically equal to *1*. In presence of spatial correlations, the probability to find a particle at a distance r away from an other particle may be enhanced or depleted leading $\eta(r)$ to be greater or lesser than *1*. The pair correlation function is also very often referred to as radial distribution function. Pair correlation function has the great advantage of providing scale by scale quantification of clustering and to allow theoretical predictions of settling velocity, coalescence... (Balkovsky et al., 2001; Falkovich et al., 2003; Falkovich and Pumir, 2004; Zaichik and Alipchenkov, 2009). Unfortunately, it is too difficult to build a single scalar quantifying the level of clustering from the pair correlation function. Nevertheless Stokes number similarity has been clearly evidenced with pair correlation analysis by Saw et al. (2008) as illustrated in Fig. 4 where pair correlation functions associated to the same averaged Stokes numbers obtained with different particles and turbulent times reasonably collapse.

3.1.1.6. Voronoï diagrams. We have recently proposed the use of Voronoï diagrams in the framework of preferential concentration/clustering. A Voronoï diagram is the unique decomposition of *nD* space into independent cells associated to each particle. One Voronoï cell is defined as the ensemble of points that are closer to a particle than to any other. From the definition of the Voronoï diagrams, it appears that the volume V of a Voronoï cell is the inverse of the local *nD*-concentration in particles; therefore the investigation of Voronoï volumes field is strictly equivalent to that of local concentration field. In addition, Voronoï volumes are naturally evaluated around each individual particle present in the field, a feature which will allow Lagrangian tracking of concentration along particle trajectories. As no length scale is *a priori* chosen, the resulting local concentration field is obtained at an intrinsic spatial resolution (which is somehow self-adapted according to the local separation between particles). PDF of Voronoï volumes can be studied and their standard deviation is directly linked to the level of clustering. Indeed, for a Poisson process in 2*D*, the standard deviation is analytically known to be equal to 0.52 ; thus if the Voronoï areas standard deviation is exceeding this value, clustering is present and this statistical quantity can be used as a global measure of clustering intensity. Fig. 5 displays results obtained from 2*D* pictures of a wind tunnel experiment. On the left panel are presented PDF of the logarithm of the normalized Voronoï area that are reasonably described with lognormal distributions. On the right panel, the parameter governing these PDFs shapes (their standard deviation) is plotted for

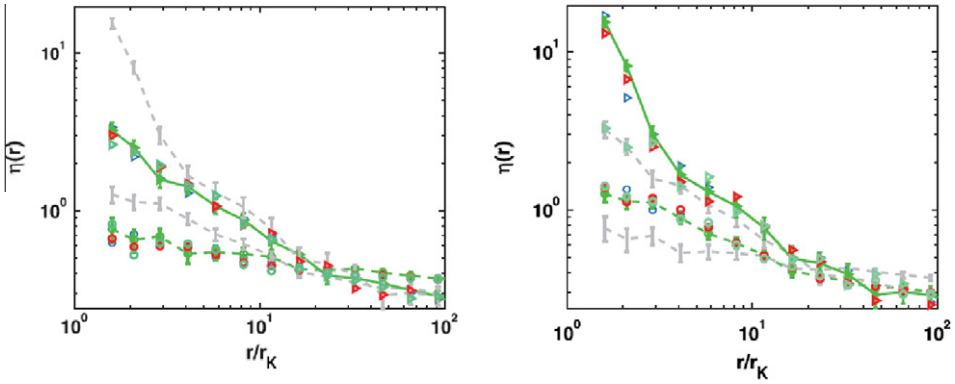

Fig. 4. Stokes similarity from experiments by Saw et al. (2008) where preferential concentration of water droplets in a wind-tunnel grid generated turbulence is investigated with pair correlation analysis. The left figure shows the Stokes similarity for droplets with Stokes numbers in the range 0.01–0.3 (circles) and 0.7–1.1 (triangles) while the right figure is for Stokes numbers if the range 0.3–0.7 (circles) and 1.1–1.5 (triangles). Light gray lines in the background are for other groups of Stokes numbers. For each range of Stokes number, the colors of the symbols correspond to different experimental conditions (different droplet size, mean wind velocity and measurement distance downstream the grid). The Stokes similarity is shown by the collapse of the pair correlation of particles within the same range of Stokes number regardless of experimental conditions. (For interpretation of the references to color in this figure legend, the reader is referred to the web version of this article.)

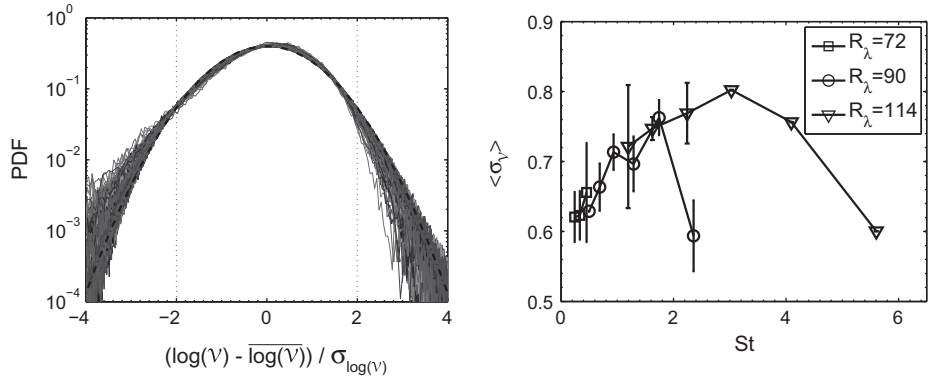

Fig. 5. Left: PDF of the logarithm of the normalized Voronoï area for 40 experiments spanning a wide range of control parameters (Stokes and Reynolds numbers, mass loading). Right: dependence of these PDF standard deviations with the Stokes number evidencing clustering intensity. Experiments from Monchaux et al. (2010).

various experiments as a function of the averaged Stokes number, evidencing a maximum clustering effect for Stokes numbers around unity. For more details see Monchaux et al. (2010).

3.1.1.7. Other methods. Reeks and co-workers have been proposing to use the full Lagrangian method (Ijzermans et al., 2009, 2010) to evaluate the compressibility of the particle phase. The idea is to follow the deformation tensor J_{ij} associated with an infinitesimally small volume of particles following the considered particle. The determinant $J = |J_{ij}|$ is the inverse of the concentration following a particle trajectory. In addition, it is shown that $d\langle \ln J\rangle/dt$ is equal to the averaged compressibility of the particle velocity field (i.e. $\nabla \cdot V_p$). Two methods are therefore available to compute J. The evaluation of $\nabla \cdot V_p$ requires a very dense seeding feasible in simulations (one-way coupling only) which is almost impossible to achieve in experiments (not withstanding the fact that the volume loading and the seeding are the same in physical experiments). The second approach based on the concentration along the particle trajectory is better adapted to experiments, in particular, and as shown by Monchaux et al. (2010), it can be implemented with the above described Voronoï analysis. In addition, that technique would also provide space-average moments of the particle concentration field to be compared with predictions (see for example Ijzermans et al. (2010) in the perspective of assessing its intermittency character and addressing the question of the existence or not of a long-term frozen state).

Namenson and collaborators have proposed to use wave number power spectra to study patterns formed from clustering (Namenson et al., 1996; Hogan et al., 1999) introduced the use of the so-called singularity spectrum to characterize the particle concentration field. They have also developed a conditional method based on the relative Stokes number dependent concentrations obtained in localized region of space Hogan and Cuzzi (2001). These approaches have not been much followed.

3.1.1.8. Dynamical approaches. An alternative method to identify preferential concentration phenomena consists in exploring particle dynamical properties and in identifying a systematic bias reminiscent of a possible preferential sampling of the carrier turbulent background. This approach is generally useful in situations where the seeding density is too low for any direct investigation of particle concentration field. However, in order to infer what the preferentially sampled regions are in terms of flow properties, the implicit assumption needs to be made that, locally, particle dynamics deviates only weakly from the fluid's one. Therefore such indirect approaches should be limited to moderately inertial particles with $St < 1$. An example of such a dynamical approach is the recent work by Gibert et al. (2010) who investigated acceleration statistics of solid inertial particles with $St < 0.5$ in a swirling von Kármán flow. Their experimental particle tracking velocimetry measurements indicate that such particles tend to preferentially concentrate in strain-dominated regions. This conclusion is

inferred from the analysis of Eulerian velocity–acceleration cross-structure function interpreted in the light of a simple model where inertial particles are assumed to follow at first order the fluid and their dynamics is described locally in terms of the fluid velocity gradients tensor. They show that their observations are consistent with a dominant intermediate eigenvalue of this tensor, corresponding to a dominant strain.

3.1.2. Associated results

From the various approaches described above, several robust findings can be identified regarding the level of clustering of heavy particles in turbulent flows. Clustering is present on at least three decades in Stokes numbers from 0.1 to several hundred in experimental configurations as well as in numerical simulations. A striking feature is the variety of numerical works that evidence clustering, regardless of the crudeness of the simulation schemes employed since we have seen that Stokes force in a point particle limit is sufficient to observe the phenomenon even in random flows or kinematic or synthetic flows. To this regard, a distinction has to be done between clustering at dissipative scales that would rely on the dissipative dynamics and clustering at inertial scales linked to interactions of particles with vortex and high strain regions of the flows (Bec et al., 2007a) or to zero-acceleration points dynamics (Coleman and Vassilicos, 2009) and more generally to the acceleration field in the vicinity of the inclusion. Thus, the different simulations type would capture different mechanisms (Chen et al., 2006; Bec et al., 2007a). Visualizations as well as any quantification attempt show that clustering appears to be particularly enhanced for particles whose Stokes numbers based on the classical definition are around unity. Box counting methods (see Fig. 2 and Aliseda et al., 2002) have evidenced a maximum effect of clustering on scales around $10\eta_K$. This estimate has also been suggested by Qureshi et al. (2008) to be compatible to interpret some size dependency trends observed for the dynamics of finite size inertial particles. Beyond these global results it is of prime interest (see for example Aliseda et al., 2002) to have insight into the possible existence of clusters as defined in our introduction and consequently there is a need for clusters identification and characterization.

3.2. Identifying and characterizing clusters/voids

Several strategies have been developed to identify and/or characterize clusters (or depleted regions) in turbulent flows from numerical or experimental data. We present here these strategies that aim at getting topological and statistical information as clusters/voids areas, perimeters, aspect ratio, size distribution, topology...

3.2.1. Strategies

3.2.1.1. Minkowski functional. An original approach has been proposed by Calzavarini et al. (2008) to geometrically characterize clusters of particles in turbulent flows. The method, already used in cosmology, consists in considering the union of balls of radius r centered on the considered set of particles. Calculating morphological indicators for this union (namely the volume, the surface, the mean curvature and the Euler characteristics) and tracking their dependence with r allows to get insight into the topological structure of the set of particles. The authors managed to evidence the filamentary and tube-like structure of bubble and heavy particle clusters respectively. Results from this approach are original, but the associated calculation time is very high. These results provide global topological indications on clustering but do not allow individual cluster identification.

3.2.1.2. Box counting methods. From the box counting methods described above, one obtains for each chosen scale r a concentration map. Following Aliseda et al. (2002), it is possible to define a concentration threshold for these maps. Connected boxes that are above the defined threshold are considered as clusters, their characteristics (area, perimeter...) are then easily calculated and studied. This method requires the choice of the appropriated scale r and of the concentration threshold which may be subjective. A similar study can be undertaken for the investigation of depleted regions. At some scale r, connected empty boxes are defined as voids. When r is small enough, that measure gives a perfect evaluation of the voids geometry and characteristics (see Goto and Vassilicos, 2006; Yoshimoto and Goto, 2007 for examples).

3.2.1.3. Minimum spanning trees. J. Bec suggested in a private communication to use minimum spanning trees to study clustering. They would allow to identify clusters easily, even if one has to set an arbitrary threshold. We have applied this method to our data, but the results (not presented here) are difficult to analyze due to this threshold issue. Moreover, it has to be noted that this method is quite demanding in terms of CPU time.

3.2.1.4. Voronoï diagrams. As presented in Monchaux et al. (2010), Voronoï diagrams can be efficiently used to identify clusters from data. Consider Fig. 6b which presents the ratio of the Voronoï PDF for a typical experiment and for a Poisson process, for low and high values of normalized Voronoï area, corresponding respectively to high and low values of the local concentration, experimental PDF is above the Poisson one, while we observe the opposite for intermediate area values. Voronoï cells whose area is smaller than the first intersection $\mathcal{V}_c$ are considered to belong to a cluster. Fig. 6 also displays a full Voronoï diagram corresponding to one image taken from one experiment. On this diagram, cells corresponding to clusters have been colored in dark gray. It appears that dark gray cells tend to be connected in groups of various sizes and shapes that are identified as clusters whenever they belong to the same connected component. This method does not require subjective choice of any threshold.

As a guide for future work, Table 1 compares the ability or efficiency regarding preferential concentration/clustering analysis of the different methods previously presented.

3.2.2. Associated results

3.2.2.1. Depleted regions and clusters. Fig. 1 has shown regions of very high and very low concentration in particles revealing the clustering of inertial particles in HIT. Regarding modeling of particle laden flows, it is of prime interest to characterize these dense and depleted regions and some of the tools we have just described may be used to do so. Box counting methods have been successfully employed to characterize voids: one chooses a small enough box size to tile the space, then one identifies as empty regions the unions of connected boxes containing no particles. Voronoï diagrams have also been employed in almost the same way (see Section 3.2.1). The results obtained from both techniques lead to the same conclusion in 2D DNS (Boffetta et al., 2004; Goto and Vassilicos, 2006), in 3D DNS (Yoshimoto and Goto, 2007) and in experimental wind tunnel (Monchaux et al., 2010) as can be seen in Fig. 7 where the PDF of the holes or depleted regions area are presented. It is always found that the holes area are distributed according to a power law with slope around -1.8 independently of the simulation/experiment and of the particle Stokes number. Similarly, clusters may be identified as connected regions where the local concentration (measured from box counting, Voronoï analysis, minimum spanning tree...) exceeds a given threshold. Associated results have been proposed by several teams working in wind tunnel experiments (Aliseda et al., 2002; Monchaux et

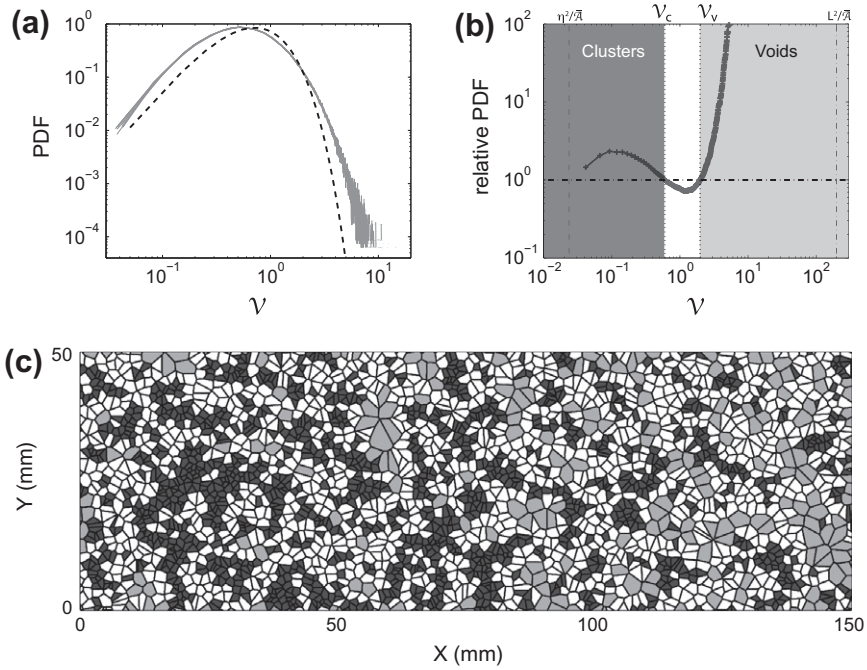

Fig. 6. A way to identify clusters: (a) Superimposition of the Voronoï areas PDF for a typical experiment ($R_\lambda = 85$, $St = 0.33$, 500 particles per image); 10 continuous lines associated to ten sets of 500 uncorrelated independent Voronoï diagrams are represented (dispersion is negligible) and a dotted line associated to random Poisson process; (b) ratio of the two PDF presented on the left figure. Vertical dash-dotted lines indicates η_K^2 (left) and L^2 (right). (c) colored visualization of clusters (dark gray) and voids (light gray). (For interpretation of the references to colour in this figure legend, the reader is referred to the web version of this article.)

Table 1
Semi quantitative evaluation of different methods regarding most relevant indicators. Note that Voronoï tessellations are so far not included in any modeling or theoretical prediction, which limit their relevance while Divergence Jacobian, correlation dimension or pair correlation function are well inserted in many theoretical approaches and connected with modeling.

	Visualizations	Clustering index	Box counting	Correlation dimension	Pair correlation	Divergence Jacobian	Voronoï	Minkowski
Computation efficiency	Excellent	Excellent	Poor	Good	Good		Good	Poor
Concentration map	No	No	Yes	No	No	No	Yes	No
PC quantification	No	Yes	Yes	Yes	Yes	Yes	Yes	No
Intrinsic resolution	Yes	No	No	Yes	Yes	No	Yes	Yes
Lagrangian tracking	No	No	Difficult	No	No	Yes	Yes	No
Clusters/holes identification	Yes	No	Difficult	No	No	No	Yes	No
Clusters/holes characterization	No	No	Difficult	No	No	No	Yes	Yes

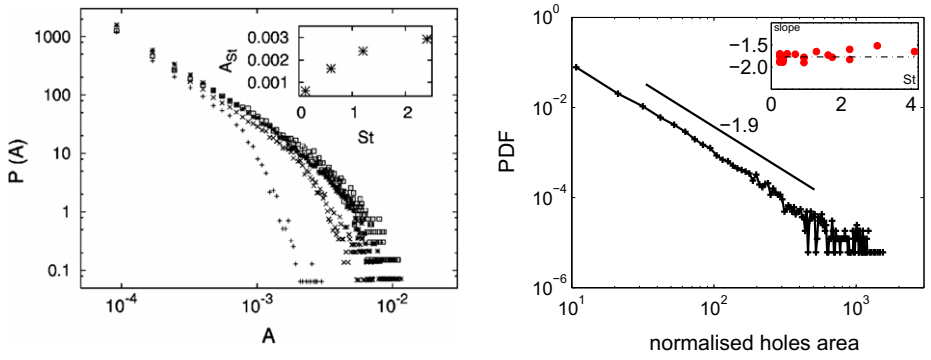

Fig. 7. PDF of holes or depleted regions areas in a 2*D* DNS on the left and 2*D* measurements in a wind tunnel experiment on the right. Pictures are respectively using box counting methods and Voronoï analysis and are taken from Boffetta et al. (2004) and Monchaux et al. (2010).

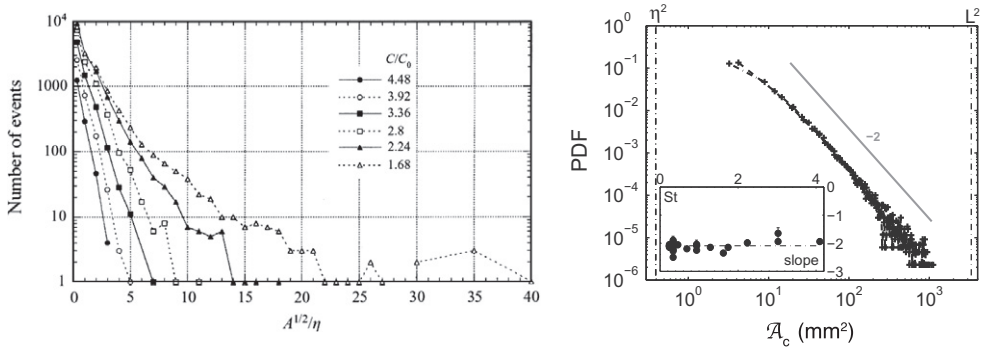

Fig. 8. PDF of clusters areas in wind tunnel experiments. Pictures are respectively using box counting methods and Voronoï analysis and are taken from Aliseda et al. (2002), Monchaux et al. (2010).

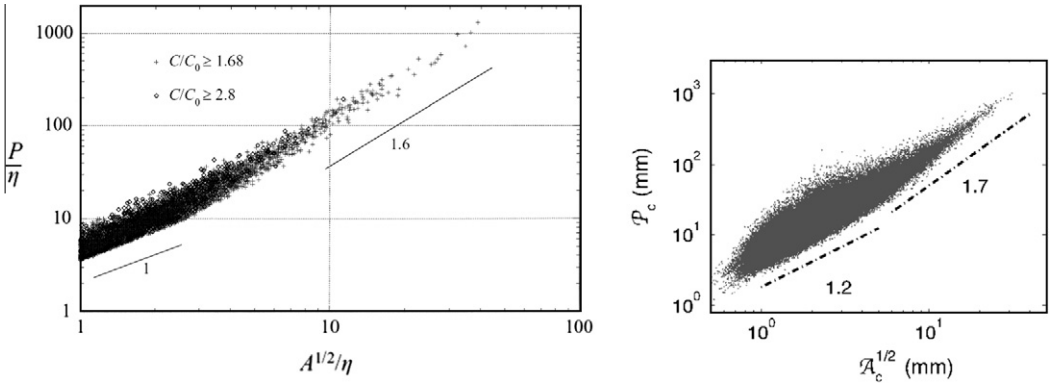

Fig. 9. Relation between clusters area and perimeter. Pictures are respectively using box counting methods and Voronoï analysis and are taken from Aliseda et al. (2002) and Monchaux et al. (2010).

al., 2010) and are presented in Fig. 8. Aliseda and coworkers suggested that the areas presented on the left figure were exponentially distributed while the right figure clearly show a power law distribution. Actually, results from the former are also compatible with a power law behavior. In this case, no typical size can be identified, and considering the small exponents (around −1.8 and −2 for holes and clusters respectively), average sizes cannot even be defined.

Regarding the clusters shapes, Minkovski functional analysis has evidenced that particles gather in interconnected empty tunnel and more precise works based on box counting or Voronoï methods show that individual clusters have fractal structures. See Fig. 9.

4. Physical mechanisms

4.1. Turbulence-particle interactions

We are mainly focusing on preferential concentration/clustering issues of heavy particles in turbulent flows. Most of the work dedicated to these studies consist of numerical simulations where back reaction of the particles on turbulence is not taken into account, and in experiments with mass and volume fraction loading that are small enough to neglect this back reaction. As a consequence the two-way coupling effects are not supposed to be relevant in these contexts and this section will only deal with the actions of the turbulent flows on the particles that enable their preferential accumulation.

4.1.1. Response to flow structures

Experimentalists have been used for a long time to seed turbulent flows with micro bubbles to visualize high shear or high vorticity regions as vortex filament for instance. In the review by Eaton and Fessler (1994) structured flows are considered in which it is easily seen that heavy particles are surrounding mixing layer or wakes vortices. The basic underlying mechanism is the following: due to their inertia, particles denser than the fluid tend to be ejected from vortical structures while they are easily trapped by convergent regions of the flow. The opposite behavior is expected for particles less dense than the carrier fluid. If these behaviors are easily seen and understood on simple steady flows, there is a wide gap to fill to directly apply them to homogeneous isotropic turbulent flows where, even if structures do exist, they do not necessarily live for long times.

There is now considerable evidence for a high correlation between, for example, regions of high strain and low vorticity and regions of high concentration in heavy particles. Squires and Eaton (1990, 1991), Wang and Maxey (1993), Vaillancourt et al. (2002), and Tanaka et al. (2002) show simultaneous visualizations of vorticity and particle concentration isocontours obtained from spatial slices of direct numerical simulations that clearly show a strong correlation between these two quantities. More quantitative analysis have of course been undertaken. They consist in representing statistics of concentration conditioned to the levels of vorticity/strain. The latter are computed from one of the many criteria existing to identify structures in turbulent flows. Squires and Eaton (1990, 1991) used a refined Q-criterion (Hunt et al., 1988) to

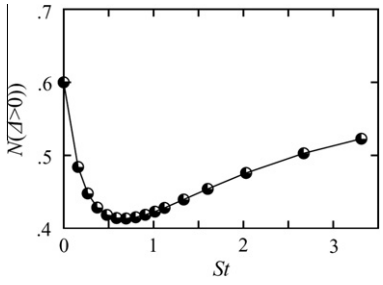

Fig. 10. Relative fraction of particles in the rotating regions as a function of St in 3*D* DNS by Bec et al. (2006). Δ is the discriminant (as defined for instance by Chong et al. (1990)): $\Delta = \left(\frac{\det[\sigma]}{2}\right)^2 - \left(\frac{\mathrm{Tr}[\sigma^2]}{6}\right)^3$, where $\sigma_{ij} = \partial_i u_j$ is the velocity gradient tensor of the flow. Regions where Δ is positive are dominated by rotation, while regions where Δ is negative are strain-dominated.

identify in their simulation of HIT eddies, rotational, streaming and convergent regions. They present particle number density distributions functions within each of these regions, showing that the average concentration in eddies is twice the global mean concentration while it is divided by a factor greater than *2* in rotational and convergent zones. Wang and Maxey (1993), plotting the average local concentration in particles as a function of the strain and vorticity, show very similar results. Fig. 10 taken from Bec et al. (2006) summarizes these results and shows that as the Stokes number gets closer to unity, the relative number of particles in rotational regions tends to decrease, indicating that heavy particles tend to live in strain-dominated regions. More recently, Calzavarini et al. (2008) using Minkowski functionals (see Section 3.2) have evidenced that heavy particles tend to cluster in interconnected empty tunnels, a picture which is compatible with the classical image of heavy particles being ejected from filamentary vortical structures that are known to be present in turbulent flows. Using dynamical tools (see Section 3.1), Gibert et al. (2010) have also deduced that small heavy particles in a von Kármán flow tend to accumulate in strain-dominated regions. Coleman and Vassilicos (2009) also used the Q-criterion calculated for the fluid and for different sets of particles with various Stokes number. They show that, when the Stokes number is large enough ($St \simeq 3$), the Okubo–Weiss parameter PDF calculated on the particles and on the fluid are indistinguishable. Similarly, by studying particle acceleration, Bec et al. (2006) suggest that at small Stokes numbers, the little particle inertia is sufficient to expel them from vortices leading to modified acceleration PDF while at higher Stokes numbers, the differences between fluid and particle acceleration PDF cannot be attributed any more to this centrifuging effect but rather to filtering of the velocity induced by the particle response time. All together, these results would imply that the effect of centrifuging usually invoked to explain clustering is not that relevant at moderately high Stokes numbers and thus there is a call for other physical mechanisms.

4.1.2. Collisions and coalescence

Preferential concentration of inertial particles is believed to potentially play an important role in enhancing particle collision rate and eventually coalescence in the case of fluid particles. Such process is for instance considered as a possible mechanism to understand rain initiation in warm clouds, where no clear explanation has emerged yet to explain the rapid growth rate of the droplets prior to rain (Shaw, 2003; Falkovich et al., 2002). In spite of decades of research, the prediction of the collision/coalescence rate C of particles in turbulence remains an open question. The usual approach consists in evaluating the flux of particles seen by each individual particle, where particles are simply advected by the carrier flow. In such conditions, the collision rate can be approximated as

$$C = \pi n_0^2 a^2 \langle |w_r|^2 \rangle, \tag{9}$$

with n_0 the local seeding density of particles, a their radius and w_r the radial relative velocity of the pair of particles. In this context, Saffman and Turner investigated the case of tracer particles, leading to $C_{ST} = 1/2 n_0^2 a^3 \left(\frac{8\pi}{15}\right)^{1/2} / \tau_\eta$ (Saffman and Turner, 1956). However, this prediction is known to fail predicting the case of inertial particles, and to significantly underestimate the actual collision rate of heavy particles in a turbulent flow. This results from two effects, related to particle accumulation properties. The first effect is directly related to the trend of inertial particles to preferentially concentrate in clusters, what locally enhances the seeding density n_0. This effect is generally modeled by introducing a corrective factor $g(a)$ in the collision rate prediction (9) to account for the corrected spatial distribution of particle pairs. The second mechanism which enhances the collision of particles is related to the *sling effect* due to the formation of caustics (Falkovich et al., 2002; Falkovich and Pumir, 2007) which correspond to regions where particle relative velocity is large. The formation of caustics has been proposed by Wilkinson et al. (2006) as a possible relevant mechanism to explain the rapid onset of rainfall from convective clouds (even in the absence of clustering of particles). How to accurately parametrize this effect in particle collisions models remains an active matter of research. Using a *ghost particle* approximation, which merely counts particle trajectories running into each other, Ducasse and Pumir (2009) have recently shown that such approximation may lead to an overestimate by as much as 30% of the collision rate in simple models of turbulent flows.

4.1.3. Sweep-stick mechanism

Vassilicos and his collaborators have elaborated along the last five years a new vision of particle clustering in HIT. In their pioneering work in 2*D* inverse cascading turbulence (Goto and Vassilicos (2006)), they show visualizations that evidence very strong correlation in a wide range of scales between distributions of heavy inertial particles on the one hand and zero-acceleration points on the other hand (see Fig. 11). Since then, they have extended their findings to 3*D* turbulence and put them on a more quantitative ground (Chen et al., 2006; Goto and Vassilicos, 2008; Coleman and Vassilicos, 2009). They first have shown using pair correlation functions that zero-acceleration points do cluster in a manner very similar to heavy inertial particles, at least at scales larger than $0.5\eta_K$ (Chen et al., 2006). Then, they have quantified these correlations computing:

$$C_b^a(r) = \frac{\Sigma_{i=1}^{N(r)} \left(n_i^a - \langle n^a \rangle\right)\left(n_i^b - \langle n^b \rangle\right)}{\left[\Sigma_{i=1}^{N(r)} \left(n_i^a - \langle n^a \rangle\right)^2 \left(n_i^b - \langle n^b \rangle\right)^2\right]^{1/2}}, \tag{10}$$

where they have divided the whole volume into $N(r)$ boxes of equal volume depending on the observation scale r, n_i^a is the number of particles of type a in a box i and $\langle n^a \rangle$ is the mean number of particles of type a in a box of size r. They defined three types of "particles": the inertial particles, the zero-acceleration points and a set called $\mathcal{A}$ gathering points where acceleration is normal to the eigenvector of the acceleration gradient tensor associated to the larger eigenvalue. In 2*D* as well as in 3*D* DNS, correlations of inertial particles position with both zero-acceleration points and $\mathcal{A}$ set particles are non-vanishing, and as the observation scale r is increased, correlations with zero-acceleration points monotonically increase while correlations with $\mathcal{A}$ saturate and eventually decrease beyond $r \simeq 10\ \eta_K$. They explain the underlying mechanisms as follows: on the one hand, zero-acceleration points are swept by the fluid as they statistically move with the local velocity of the fluid. On the other hand,

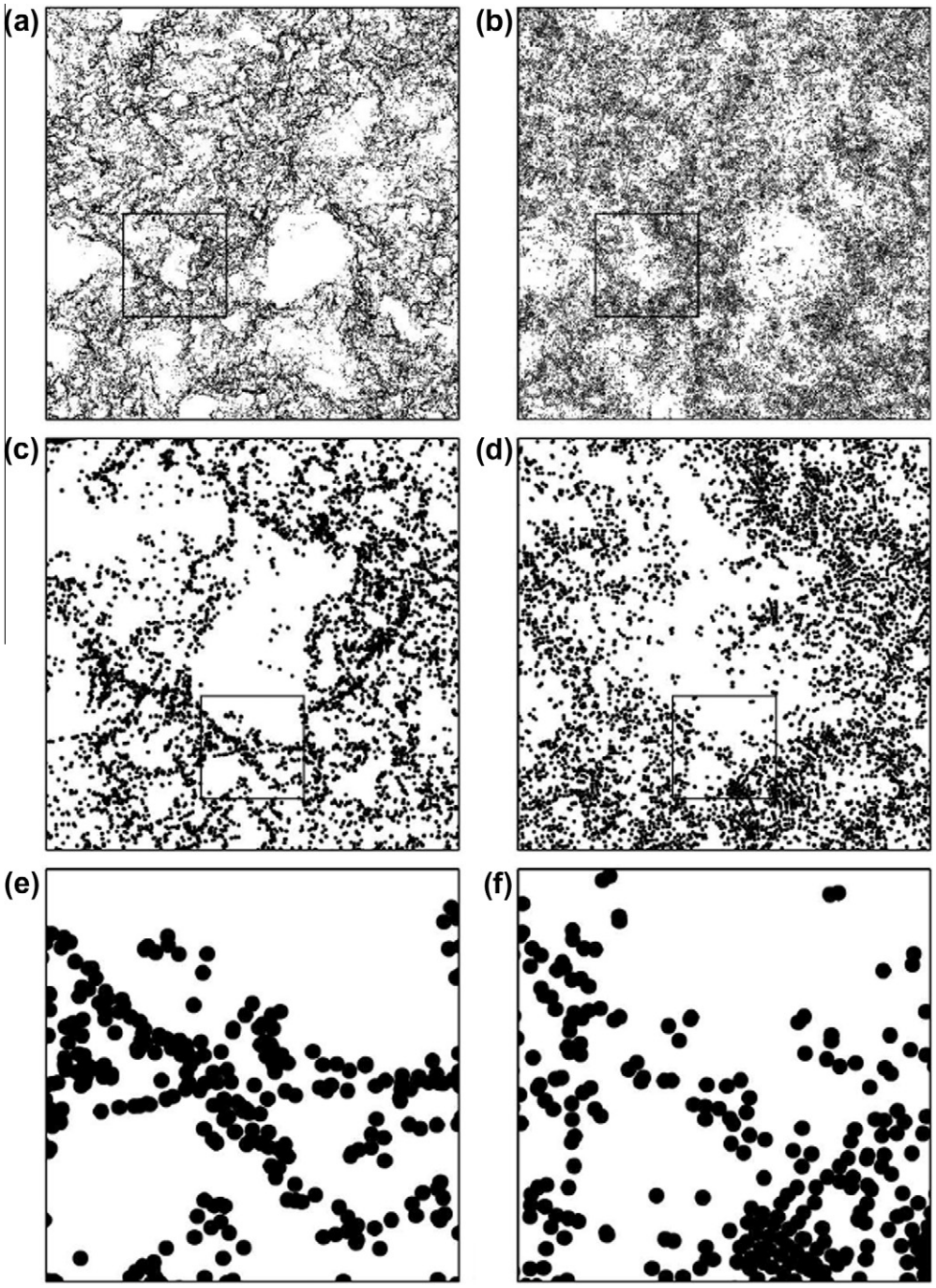

Fig. 11. (a, c, and e) Spatial distribution of inertial particles with St = 1.9. (b, d, and f) Spatial distribution of zero-acceleration points. (a and b) The side length of plots is about 7 integral scales corresponding to 200 Kolmogorov scale. (c and d) The four-times magnification of squared region in (a and b). (e and f) The four-times magnification of squared region in (c and d). Taken from Goto and Vassilicos (2006).

they show that a heavy particle that meets a zero-acceleration point moves with the fluid velocity, which is no longer true when the particle is at a point with nonzero acceleration. They refer to this as the sticky part of the mechanism. Recently, experimental measurements in a wind tunnel (Monchaux et al. (2010)) have evidenced behaviors compatible with this mechanism. Using Voronoï tessellation, the authors have shown that maximum of preferential concentration is observed for Stokes number around unity while sizes and shapes of clusters (considered as regions where the local concentration exceeds a given threshold) do not depend on the Stokes number (and as seen in Section 3.2.2, a similar behavior is found for holes or depleted areas). This apparent discrepancy vanishes when considering the average concentration within clusters that depends on Stokes number at second order. These three facts may be linked to the sweep-stick framework: the shapes and sizes of particle clusters are directly governed by the distribution of zero-acceleration points that is independent of Stokes number while the concentration within clusters depends on it through the sticky part of the mechanism.

4.2. Settling velocity

In the presence of gravity, and as anticipated by Maxey and Corrsin (1980), it has been observed in simulations (Wang and

Maxey, 1993) and in experiments (Aliseda et al., 2002) that particle interactions with turbulent structures tend to enhance the settling velocity of these particles. The commonly accepted basic underlying mechanism relies on the fact that falling particles tend to be systematically swept toward the downward side of turbulent eddies (Wang and Maxey, 1993), a proposal consistent with the fact that the velocity enhancement is maximum at a Stokes number close to unity. In a more extensive investigation using LES, Yang and Lei (1998) have shown that the maximum of the velocity enhancement also depends on the Rouse number and that it evolves somewhat with the turbulent Reynolds number. Yet, the above mentioned simple qualitative mechanism fails to explain the experiments by Aliseda et al. (2002) which have shown that the settling velocity of water droplets in a grid generated turbulence is further enhanced when the seeding density is increased (all others parameters being unchanged), and even in relatively diluted suspensions where the background turbulence is not significantly modulated by the dispersed phase. Their measurements reveal the key role of collective effects as the fall velocity conditional on the local concentration was found to linearly increase with the latter, and that this trend holds irrespective of the Stokes number considered. Their idea was that the increase on the fall velocity results from the combination of both individual and collective behaviors. The former arises in dilute conditions according to Maxey's view, while the collective effect was mainly due to the enhancement of momentum coupling between phases that took place in regions of high concentration. By treating clusters like dense pseudo-particles falling within gravity, they recovered the magnitude of the velocity enhancement as well as its observed linearity with the local concentration. That view was further supported by the numerical simulations of Tanaka et al. (2000) and of Bosse et al. (2006) who both considered a two-way coupling approach, *i.e.* precisely incorporating the momentum exchange between phases. They found that the fall velocity is indeed enhanced compared with the case of particles simply responding to turbulence solicitations (one-way coupling), and also that the velocity increase is almost linear with the (average) volume loading. Similar findings were obtained by Wang et al. (2007) using a different numerical approach. More recently, Zaichik and Alipchenkov (2009) and Alipchenkov and Zaichik (2009) developed a model that combines Batchelor theory for sedimenting spheres with an approximate solution of the radial distribution function for finite inertia particles assuming a Gaussian random process for the turbulent velocity increments. Their predictions happen to be in fairly good agreement with Aliseda et al. findings although the magnitude of the velocity enhancement is overestimated, possibly because the influence of gravity was not accounted for. Clearly, some discrepancies persist between experiments and simulations as well as the available theory on the magnitude of the velocity enhancement. The scaling of this effect when varying the turbulent Reynolds number is also worth investigating further, as well as the case of particles larger than the Kolmogorov length scale. Better understanding of these collective mechanisms is certainly one important contemporary challenge in the field of inertial particles in turbulence, in particular regarding its consequences on the coalescence efficiency.

5. Expected future breakthrough

5.1. Experimental and numerical challenges

To better understand particle-turbulence interactions, simultaneous measurements of the fluid field (with all turbulent scales fully resolved) and of the (finite size) particle dynamics are clearly required. For dilute conditions, significant progresses have been achieved in that direction which are mostly based on 2D imaging (see for example (Yang and Shy, 2005; Poelma et al., 2006; Zhou and Chang, 2009), with some contributions now emerging on imaging 3D fields (for example Guala et al., 2008 used combined PTV techniques and Gibert (2011) imaged big water gel droplets). A further step would be to perform such measurements in denser systems, possibly including an investigation of the flow field structure within clusters (that may be useful for phase coupling) and also at higher turbulent Reynolds numbers. Measurements in globally or locally dense conditions are clearly an enormous challenge. For optically thick systems, new measuring techniques will be required. New possibilities can emerge from high speed X-ray tomography, for which high temporal resolution has recently been achieved (Liu et al., 2009) recently achieved temporal resolution of the order of microsecond), while the spatial resolution still lags behind the objective, or from magnetic resonance imaging for which the temporal resolution is still an issue (see for example the review by Werth et al., 2010). For these techniques, one can expect developments similar to those achieved for imaging in the visible range, in particular concerning X-ray particle tracking velocimetry.

Concerning simulations, and as exemplified throughout this paper, our knowledge of dispersed two-phase flows has significantly improved based on the point particle approximation. Accounting for the finite size of particles constitutes now the current challenge, in particular because accumulating pieces of information converge toward the need for distinguishing between the influence of the particle size and of its density. A number of numerical schemes have been developed that already bring new insight on the dynamics of isolated particles, including particularly the modification of the turbulent field in the vicinity of the inclusion, the instantaneous force and torque acting on it, the interaction of its wake with the turbulent field... (see Bagchi and Balachandar, 2003; Burton and Eaton, 2005; Naso and Prosperetti, 2010; Homann and Bec, 2010; Zeng et al., 2010 for some recent contributions). Simulating many freely moving inclusions in a turbulent environment is an even more challenging task. Very promising contributions based on a variety of numerical methods are already available (Ten Cate et al., 2004; Zhang and Prosperetti, 2005; Uhlmann, 2008; Yeo et al., 2010; Lucci et al., 2010, 2011), some of which allowing to follow four to six thousands finite size particles while resolving all scales. Such numerical approaches are expected to drastically expand in the near future (Tryggvason, 2010) and they will indubitably help clarifying some other open issues.

5.2. Physical insight

Concerning clustering, the influence of the dispersed phase loading is to be analyzed in more detail. For example, the non linear increase of the concentration within clusters with the average loading reported by Monchaux et al. (2010) remains unexplained, and one may wonder if that behavior changes with the turbulent Reynolds number. Others open issues concern the characterization of collective effects that take place in these systems, in particular with respect to the coupling between phases including the modulation of the turbulence (see the review by Poelma and Ooms, 2006) and to the enhancement of the settling velocity in relation with the RDF dependence... The respective role of volume and mass loadings is also worth to be clarified.

Another open question concerns the time needed to form clusters or to destroy them. That issue is of interest in a number of applications, and notably in combustion, and it is not settled although some estimates are available from simulations (Wang and Maxey, 1993). Experiments in that respect are very difficult but, following an observation by Fallon and Rogers, some useful information may possibly be collected using a controlled change

in the external body force (possibly using charged particles in electric fields). Simulations should decisively help in that matter.

A crucial issue lies in the behavior of particles much larger than Kolmogorov length scale. Not so many well controlled experiments or simulations are available today for such conditions and there is thus ample room for new investigations aimed at unveiling fundamental mechanisms. For example, the influence of the finite size of particles on the modulation of turbulence is on the way to be clarified for moderate particle Reynolds number inclusions (Lucci et al., 2011) but more is needed concerning wake-turbulence interactions (Zeng et al., 2010). In the same perspective, the interaction between a background turbulent field and the so-called particle-induced turbulence, the latter arising either from interacting wakes (Hunt and Eames, 2002; Riboux et al., 2010) or from particle-particle interactions (Cartellier et al., 2009) is still poorly understood.

In the context of the dynamics of individual particles, Lagrangian statistics have been very early identified as key quantities to understand the underlying coupling with the carrier turbulent flow. They are receiving much attention nowadays as they are becoming accessible thanks to development of experimental and simulation techniques, which allow to carefully investigate the forcing exerted by the turbulent field on the particle. These investigations are particularly important for the implementation of relevant 1-way coupling models for the particle equation of motion beyond the usual point particle approximation (Maxey and Riley, 1983; Gatignol, 1983). Concerning clustering and preferential concentration issues, Lagrangian statistics have also been recently identified as potentially important. For instance, recent measurements of settling velocity by Aliseda et al. (2002) have shown the existence of collective effects, resulting in a enhancement of the settling velocity of clustered particles. The modeling of such collective effects may be improved if quantities such as the local concentration field along particle trajectories and the typical residence time of particles inside the clusters, could be quantified. Such residence time measurements were attempted by Aliseda et al. (2002) using LDA time series, but the trends were not clear enough to be exploited. Measurements of the concentration along a given particle trajectory (which are by essence Lagrangian), which have been initiated by Monchaux et al. (2010), are expected to produce more reliable statistics, and thus should open the way to a better understanding of the role of clusters on particle dispersion and on settling velocity enhancement. In this context, accessing Lagrangian statistics of the particle dynamics (velocity and acceleration) conditioned to the local concentration along their trajectories remains an important challenge. Let us indeed recall that the concentration seen by the particles along their trajectory gives access to the deformation tensor of particle positions: that Lagrangian variable is related to the particle compressibility and thus to the underlying acceleration field (see Coleman and Vassilicos, 2009). Such a program is under way at LEGI (France) particularly with the aim to evaluate the intermittency of the particle number density.

Dynamical clusters tracking is a far more complex issue, much more difficult to achieve with present tools. As mentioned in the introduction, important aspects for modeling and practical applications are the existence of clusters and the study of their dynamical behavior. Using Voronoï diagrams for example, one can easily identify clusters in 3D flows, the next step being to follow them to get access to relevant quantities as the residence time of particles, the dependence of their inner concentration and of their geometrical characteristics. To tackle these issues, it is required to have access to large numbers of particles (at least hundreds of thousands) in three dimensional flows. So far, no experimental facility can achieve these requirements because of the measurement sensitivity to particle gains or losses using 2D illumination systems and numerical simulations have to be employed.

All the new understanding arising from such investigations should benefit two-phase flow modeling and ultimately simulations useful for engineers.

References

Ahmed, A.M., Elghobashi, S., 2001. Direct numerical simulation of particle dispersion in homogeneous turbulent shear flows. Phys. Fluids 13, 3346–3364.

Alipchenkov, V., Zaichik, L., 2009. Effect of particle clustering on the gravitational settling velocity in homogeneous turbulence. Fluid Dynam. 44, 397–404.

Aliseda, A., Cartellier, A., Hainaux, F., Lasheras, J.C., 2002. Effect of preferential concentration on the settling velocity of heavy particles in homogeneous isotropic turbulence. J. Fluid Mech. 468, 77–105.

Aly, A., Nicolleau, F., 2008. Dispersion of heavy particle sets in isotropic turbulence using kinematic simulation. Phys. Rev. E 78, 016310.

Ayyalasomayajula, S., Gylfason, A., Collins, L.R., Bodenschatz, E., Warhaft, Z., 2006. Lagrangian measurements of inertial particle accelerations in grid generated wind tunnel turbulence. Phys. Rev. Lett. 97, 144507.

Bagchi, P., Balachandar, S., 2003. Effect of turbulence on the drag and lift of a particle. Phys. Fluids 15, 3496–3513.

Balachandar, S., Eaton, J.K., 2010. Turbulent dispersed multiphase flow. Annu. Rev. Fluid Mech. 42, 111–133.

Balkovsky, E., Falkovich, G., Fouxon, A., 2001. Intermittent distribution of inertial particles in turbulent flows. Phys. Rev. Lett. 86, 2790–2793.

Bec, J., 2005. Multifractal concentrations of inertial particles in smooth random flows. J. Fluid Mech. 528, 255–277.

Bec, J., Biferale, L., Boffetta, G., Celani, A., Cencini, M., Lanotte, A., Musacchio, S., Toschi, F., 2006. Acceleration statistics of heavy particles in turbulence. J. Fluid Mech. 550, 349–358.

Bec, J., Biferale, L., Cencini, M., Lanotte, A., Musacchio, S., Toschi, F., 2007a. Heavy particle concentration in turbulence at dissipative and inertial scales. Phys. Rev. Lett. 98, 084502.

Bec, J., Biferale, L., Cencini, M., Lanotte, A.S., Toschi, F., 2010. Intermittency in the velocity distribution of heavy particles in turbulence. J. Fluid Mech. 646, 527–536.

Bec, J., Celani, A., Cencini, M., Musacchio, S., 2005. Clustering and collisions of heavy particles in random smooth flows. Phys. Fluids 17, 073301.

Bec, J., Cencini, M., Hillerbrand, R., 2007b. Clustering of heavy particles in random self-similar flow. Phys. Rev. E 75, 025301.

Bec, J., Cencini, M., Hillerbrand, R., Turitsyn, K., 2008. Stochastic suspensions of heavy particles. Phys. D Nonlinear Phenom. 237, 2037–2050.

Bodenschatz, E., 2009. Tech. rep., Max Planck Institute, Goettingen <http://www.euhit.org/i-gtf.html>.

Boffetta, G., de Lillo, F., Gamba, A., 2004. Large scale inhomogeneity of inertial particles in turbulent flows. Phys. Fluids 16, L20–L23.

Bosse, T., Kleiser, L., Meiburg, E., 2006. Small particles in homogeneous turbulence: settling velocity enhancement by two-way coupling. Phys. Fluids 18, 027102.

Brown, G.L., Roshko, A., 1974. On density effects and large structure in turbulent mixing layers. J. Fluid Mech. 64, 775–816.

Burton, T., Eaton, J., 2005. Fully resolved simulations of particle turbulence interaction. J. Fluid Mech. 545, 67–111.

Calzavarini, E., Kerscher, M., Lohse, D., Toschi, F., 2008. Dimensionality and morphology of particle and bubble clusters in turbulent flow. J. Fluid Mech. 607, 13–24.

Calzavarini, E., Volk, R., Bourgoin, M., Lév êque, E., Pinton, J., Toschi, F., 2009. Acceleration statistics of finite-sized particles in turbulent flow: the role of Faxén forces. J. Fluid Mech. 630, 179.

Cartellier, A., Andreotti, M., Sechet, P., 2009. Induced agitation in homogeneous bubbly flows at moderate particle Reynolds number. Phys. Rev. E 80, 065301.

Chareyron, D., 2009. Developpement de methodes instrumentales en vue de l'etude Lagrangienne de l'evaporation dans une turbulence homogene isotrope. Ph.D. thesis, Ecole Centrale de Lyon, France.

Chein, R., Chung, J., 1988. Simulation of particle dispersion in a two-dimensional mixing layer. Am. Inst. Chem. Eng. J. 34, 946–954.

Chen, L., Goto, S., Vassilicos, J.C., 2006. Turbulent clustering of stagnation points and inertial particles. J. Fluid Mech. 553, 143–154.

Chong, M.S., Perry, A.E., Cantwell, B.J., 1990. A general classification of three-dimensional flow fields. Phys. Fluids 2, 765–777.

Chung, J., Troutt, T., 1988. Simulation of particle dispersion in an axisymmetric jet. J. Fluid Mech. 186, 199–222.

Coleman, S.W., Vassilicos, J.C., 2009. A unified sweep-stick mechanism to explain particle clustering in two- and three-dimensional homogeneous, isotropic turbulence. Phys. Fluids 21, 113301.

Collins, L.R., Keswani, A., 2004. Reynolds number scaling of particle clustering in turbulent aerosols. New J. Phys. 6, 119.

Crowe, C.T., Chung, J.N., Troutt, T.R., 1988. Particle mixing in free shear flows. Prog. Energy Combust. Sci. 14, 171–194.

Crowe, C.T., Gore, R.A., Troutt, T.R., 1985. Particle dispersion by coherent structures in free shear flows. Particul. Sci. Technol.: Int. J. 3, 149–158.

Damaschke, N., Nobach, H., Tropea, C., 2002. Optical limits of particle concentration for multi dimensional particle sizing techniques in fluid mechanics. Exp. Fluids 32, 143–152.

Dietzel, M., Sommerfeld, M., 2010. LBM simulations on agglomerate transport and deposition. In: Proc 6th International Symposium on multiphase Flow, Heat

Transfer and Energy conversion, in AIP Conference Proceedings. vol. 1207. pp. 796–801.
Druzhinin, O.A., Elghobashi, S., 1999. On the decay rate of isotropic turbulence laden with microparticles. Phys. Fluids 11, 602–610.
Ducasse, L., Pumir, A., 2009. Inertial particle collisions in turbulent synthetic flows: quantifying the sling effect. Phys. Rev. E 80.
Eaton, J.K., Fessler, J.R., 1994. Preferential concentration of particles by turbulence. Int. J. Multiphase Flow 20, 169–209.
Elghobashi, S., Truesdell, G.C., 1992. Direct simulation of particle dispersion in a decaying isotropic turbulence. J. Fluid Mech. 242, 655–700.
Falkovich, G., Fouxon, A., Stepanov, M., 2003. Statistics of Turbulence-Induced Fluctuations of Particle Concentration. Kluwer Academic, Dordrecht, pp. 155–158.
Falkovich, G., Fouxon, A., Stepanov, M.G., 2002. Acceleration of rain initiation by cloud turbulence. Nature 419, 151–154.
Falkovich, G., Pumir, A., 2004. Intermittent distribution of heavy particles in a turbulent flow. Phys. Fluids 16, L47–L50.
Falkovich, G., Pumir, A., 2007. Sling effect in collisions of water droplets in turbulent clouds. J. Atmos. Sci. 64, 4497.
Fallon, T., Rogers, C.B., 2002. Turbulence-induced preferential concentration of solid particles in microgravity conditions. Exp. Fluids 33, 233–241.
Ferrante, A., Elghobashi, S., 2003. On the physical mechanisms of two-way coupling in particle-laden isotropic turbulence. Phys. Fluids 15, 315–329.
Fessler, J.R., Kulick, J.D., Eaton, J.K., 1994. Preferential concentration of heavy particles in a turbulent channel flow. Phys. Fluids 6, 3742–3749.
Friedman, P.D., Katz, J., 2002. Mean rise rate of droplets in isotropic turbulence. Phys. Fluids 14, 3059–3073.
Gatignol, R., 1983. The Faxen formulae for a rigid particle in an unsteady non-uniform Stokes flow. J. Méc. Théorique Appl. 2, 143–160.
Gibert, M., 2011. private communication.
Gibert, M., Xu, H., Bodenschatz, E., 2010. Where do heavy particles go in a turbulent flow? ArXiv e-prints, arXiV:1002.3755v2.
Goepfert, C., Marié, J., Chareyron, D., Lance, M., 2010. Characterization of a system generating a homogeneous isotropic turbulence field by free synthetic jets. Exp. Fluids 48, 809–822.
Goto, S., Vassilicos, J.C., 2006. Self-similar clustering of inertial particles and zero-acceleration points in fully developed two-dimensional turbulence. Phys. Fluids 18, 115103.
Goto, S., Vassilicos, J.C., 2008. Sweep-stick mechanism of heavy particle clustering in fluid turbulence. Phys. Rev. Lett. 100, 054503.
Guala, M., Liberzon, A., Hoyer, K., Tsinober, A., Kinzelbach, W., 2008. Experimental study on clustering of large particles in homogeneous turbulent flow. J. Turbul. 9, 34.
Gualtieri, P., Picano, F., Casciola, C.M., 2009. Anisotropic clustering of inertial particles in homogeneous shear flow. J. Fluid Mech. 629, 25.
Hoelzer, A., Sommerfeld, M., 2006. Transport of non-spherical particles in turbulence: application of the LBM. In: Proc. ASME Fluids Eng. Div. Summer Conf., vol. 1 of A and B. pp. 1739–1743.
Hogan, R.C., Cuzzi, J.N., 2001. Stokes and Reynolds number dependence of preferential particle concentration in simulated three-dimensional turbulence. Phys. Fluids 13, 2938–2945.
Hogan, R.C., Cuzzi, J.N., Dobrovolskis, A.R., 1999. Scaling properties of particle density fields formed in simulated turbulent flows. Phys. Rev. E 60, 1674–1680.
Homann, H., Bec, J., 2010. Finite-size effects in the dynamics of neutrally buoyant particles in turbulent flow. J. Fluid Mech. 651, 81–91.
Hong, M., Cartellier, A., Hopfinger, E., 2004. Characterization of phase detection optical probes for the measurement of the dispersed phase parameters in sprays. Int. J. Multiphase Flow 30 (6), 615–648
Hunt, J., Eames, I., 2002. The disappearance of laminar and turbulent wakes in complex flows. J. Fluid Mech. 457, 111–132.
Hunt, J.C.R., Wray, A.A., Moin, P., 1988. Eddies, streams, and convergence zones in turbulent flows. In: Studying Turbulence Using Numerical Simulation Databases, vol. 2. pp. 193–208.
Hwang, W., Eaton, J.K., 2004. Creating homogeneous and isotropic turbulence without a mean flow. Exp. Fluids 36, 444–454.
Ijzermans, R.H.A., Meneguz, E., Reeks, M.W., 2010. Segregation of particles in incompressible random flows: singularities, intermittency and random uncorrelated motion. J. Fluid Mech. 653, 99–136.
Ijzermans, R.H.A., Reeks, M.W., Meneguz, E., Picciotto, M., Soldati, A., 2009. Measuring segregation of inertial particles in turbulence by a full Lagrangian approach. Phys. Rev. E 80, 015302.
Jin, G., He, G.-W., Wang, L.-P., 2010. Large-eddy simulation of turbulent collision of heavy particles in isotropic turbulence. Phys. Fluids 22.
Kada, H., Hanratty, T., 1960. Effects of solids on turbulence in a fluid. AICHE J., 624–630.
Kobayashi, H., Masutani, S.M., Azuhata, S., Morita, S., 1992. Particle dispersion in a plane mixing layer with streamwise pressure gradient. JSME Int. J. 35, 29–37.
Kraichnan, R.H., 1968. Small-scale structure of a scalar field convected by turbulence. Phys. Fluids 11, 945–953.
Lazaro, B.J., Lasheras, J.C., 1992. Particle dispersion in the developing free shear layer. I – Unforced flow. II – Forced flow. J. Fluid Mech. 235, 143–221.
Liu, X., Im, K.-S., Wang, J., Tate, M., Ercan, A., Schuette, D., Gruner, S., 2009. Four dimensional visualisation of highly transient fuel sprays by microsecond quantitative X-ray tomography. Appl. Phys. Lett. 94, 084101.
Longmire, E.K., Eaton, J.K., 1992. Structure of a particle-laden round jet. J. Fluid Mech. 236, 217–257.
Lu, J., Nordsiek, H., Shaw, R., 2010. Clustering of settling charged particles in turbulence: theory and experiments. New J. Phys. 12, 123030.
Lucci, F., Ferrante, A., Elghobashi, S., 2010. Modulation of isotropic turbulence by particles of Taylor length-scale size. J. Fluid Mech. 650, 5.
Lucci, F., Ferrante, A., Elghobashi, S., 2011. Is Stokes number an appropriate indicator for turbulence modulation by particles of Taylor-length-scale size? Phys. Fluids 23, 025101.
Luthi, B., 2003. Some Aspects of Strain, Vorticity and Material Element Dynamics as Measured with 3D Particle Tracking Velocimetry in a Turbulent Flow. Ph.D. thesis, ETH. Znrich.
Maxey, M., Corrsin, S., 1980. Stokes spheres falling under gravity in cellular flow-fields. Bull. APS 25, paper EA6.
Maxey, M.R., 1987a. The gravitational settling of aerosol particles in homogeneous turbulence and random flow fields. J. Fluid Mech. 174, 441–465.
Maxey, M.R., 1987b. The motion of small spherical particles in a cellular flow field. Phys. Fluids 30, 1915–1928.
Maxey, M.R., Corrsin, S., 1986. Gravitational settling of aerosol particles in randomly oriented cellular flow fields. J. Atmos. Sci. 43, 1112–1134.
Maxey, M.R., Riley, J.J., 1983. Equation of motion for a small rigid sphere in a nonuniform flow. Phys. Fluids 26, 883–889.
Mei, R., 1996. Velocity fidelity of flow tracer particles. Exp. Fluids 22, 1–13.
Monchaux, R., Bourgoin, M., Cartellier, A., 2010. Preferential concentration of heavy particles: a Voronoi analysis. Phys. Fluids 22, 103304.
Namenson, A., Antonsen Jr., T.M., Ott, E., 1996. Power law wave number spectra of fractal particle distributions advected by flowing fluids. Phys. Fluids 8, 2426–2434.
Naso, A., Prosperetti, A., 2010. The interaction between a solid particle and a turbulent flow. New J. Phys. 12, 033040.
Olla, P., 2010. Preferential concentration versus clustering in inertial particle transport by random velocity fields. Phys. Rev. E 81, 016305.
Poelma, C., Dickson, W.B., Dickinson, M.H., 2006. Time-resolved reconstruction of the full velocity field around a dynamically-scaled flapping wing. Exp. Fluids 41, 213–225.
Poelma, C., Ooms, G., 2006. Particle-turbulence interaction in a homogeneous, isotropic turbulent suspension. Appl. Mech. Rev. 59, 78.
Poelma, C., Westerweel, J., Ooms, G., 2007. Particlefluid interactions in grid-generated turbulence. J. Fluid Mech. 589, 315–351.
Qureshi, N.M., Arrieta, U., Baudet, C., Cartellier, A., Gagne, Y., Bourgoin, M., 2008. Acceleration statistics of inertial particles in turbulent flow. Eur. Phys. J. B 66, 531–536.
Qureshi, N.M., Bourgoin, M., Baudet, C., Cartellier, A., Gagne, Y., 2007. Turbulent transport of material particles: an experimental study of finite size effects. Phys. Rev. Lett. 99, 184502.
Reade, W.C., Collins, L.R., 2000. Effect of preferential concentration on turbulent collision rates. Phys. Fluids 12, 2530–2540.
Riboux, G., Risso, F., Legendre, D., 2010. Experimental characterization of the agitation generated by bubbles rising at high Reynolds number. J. Fluid Mech. 643, 509–539.
Saffman, P.G., Turner, J.S., 1956. On the collision of drops in turbulent clouds. J. Fluid Mech. 1.
Saito, T., Matsuda, K., Ozawa, Y., Oishi, S., Aoshima, S., 2009. Measurement of tiny droplets using a newly developed optical fibre probe micro-fabricated by a femtosecond pulse laser. Meas. Sci. Technol. 20, 114002.
Salazar, J.P.L.C., De Jong, J., Cao, L.J., Woodward, S.H., Meng, H., Collins, L.R., 2008. Experimental and numerical investigation of inertial particle clustering in isotropic turbulence. J. Fluid Mech. 600, 245–256.
Saw, E.W., Shaw, R.A., Ayyalasomayajula, S., Chuang, P.Y., Gylfason, Á., 2008. Inertial clustering of particles in high-Reynolds-number turbulence. Phys. Rev. Lett. 100, 214501.
Schmitt, F.G., Seuront, L., 2008. Intermittent turbulence and copepod dynamics: increase in encounter rates through preferential concentration. J. Marine Syst. 70, 263–272.
Shaw, R.A., 2003. Particle-turbulence interactions in atmospheric clouds. Annu. Rev. Fluid Mech. 35, 183–227.
Shaw, R.A., Kostinski, A.B., Larsen, M.L., 2002. Towards quantifying droplet clustering in clouds. Quart. J. Roy. Meteorol. Soc. 128, 1043–1057.
Siebert, H., Gerashchenko, S., Gylfason, A., Lehmann, K., Collins, L., Shaw, R., Warhaft, Z., 2010. Towards understanding the role of turbulence on droplets in clouds: in situ and laboratory measurements. Atmos. Res. 97, 426–443.
Soldati, A., Marchioli, C., 2009. Physics and modelling of turbulent particle deposition and entrainment: review of a systematic study. Int. J. Multiphase Flow 35, 827–839.
Squires, K.D., Eaton, J.K., 1990. Particle response and turbulence modification in isotropic turbulence. Phys. Fluids 2, 1191–1203.
Squires, K.D., Eaton, J.K., 1991. Preferential concentration of particles by turbulence. Phys. Fluids 3, 1169–1178.
Tanaka, M., Komai, N., Maeda, Y., Hagiwara, Y., 2000. Two-way coupling effect on the settling velocity of small heavy particles in homogeneous turbulence . In: et al., C.D. (Ed.), Advances in Turbulence VIII, Proc. 8th European Turbulence Conference. CIMNE, Barcelona.
Tanaka, M., Maeda, Y., Hagiwara, Y., 2002. Turbulence modification on a homogeneous turbulent shear flow laden with small heavy particles. Int. J. Heat Fluid Flow 23, 615–626.
Tang, L., Wen, F., Yang, Y., Crowe, C.T., Chung, J.N., Troutt, T.R., 1992. Self-organizing particle dispersion mechanism in a plane wake. Phys. Fluids 4, 2244–2251.

Ten Cate, A., Derksen, J., Portela, L., van den Akker, H., 2004. Fully resolved simulations of colliding monodisperse spheres in forced isotropic turbulence. J. Fluid Mech. 519, 233–271.

Tryggvason, G., 2010. Virtual motion of real particles. J. Fluid Mech. 650, 1–4.

Uhlmann, M., 2008. Interface-resolved direct numerical simulation of vertical particulate channel flow in the turbulent regime. Phys. Fluids 20, 053305.

Vaillancourt, P.A., Yau, M.K., Bartello, P., Grabowski, W.W., 2002. Microscopic approach to cloud droplet growth by condensation. Part II: Turbulence, clustering, and condensational growth. J. Atmos. Sci. 59, 3421–3435.

Vinkovic, I., Doppler, D., Lelouvetel, J., Buffat, M., 2011. Direct numerical simulation of particle interaction with ejections in turbulent channel flows. Int. J. Multiphase Flow 37, 187–197.

Wang, L.-P., Ayal, Grabowski, W., 2007. Effects of aerodynamic interactions on the motion of heavy particles in a bidisperse suspension. J. Turbul. 8, 25.

Wang, L.P., Maxey, M.R., 1993. Settling velocity and concentration distribution of heavy particles in homogeneous isotropic turbulence. J. Fluid Mech. 256, 27–68.

Wang, Q., Squires, K., 1996. Large eddy simulation of particle-laden turbulent channel flow. Phys. Fluids 8, 1207–1223.

Wen, F., Kamalu, N., Chung, J., Crowe, C., Troutt, T., 1992. Particle dispersion by vortex structures in plane mixing layers. Trans. ASME J. Fluids Eng. 114, 657–666.

Werth, C., Zhang, C., Brusseau, M., Oostrom, M., Baumann, T., 2010. A review of non-invasive imaging methods and applications in contaminant hydrogeology research. J. Contam. Hydrol. 113, 1–24.

Wilkinson, M., Mehlig, B., Bezuglyy, V., 2006. Caustic activation of rain showers. Phys. Rev. Lett. 97, 048501.

Xu, H., Bodenschatz, E., 2008. Motion of inertial particles with size larger than Kolmogorov scale in turbulent flows. Phys. D: Nonlinear Phenom. 237, 2095–2100.

Yang, C.Y., Lei, U., 1998. The role of the turbulent scales in the settling velocity of heavy particles in homogeneous isotropic turbulence. J. Fluid Mech. 371, 179–205.

Yang, T.S., Shy, S.S., 2005. Two-way interaction between solid particles and homogeneous air turbulence: particle settling rate and turbulence modification measurements. J. Fluid Mech. 526, 171–216.

Yeo, K., Dong, S., Climent, E., Maxey, M., 2010. Modulation of homogeneous turbulence seeded with finite size bubbles and particles. Int. J. Multiphase Flow 36, 221–233.

Yoshimoto, H., Goto, S., 2007. Self-similar clustering of inertial particles in homogeneous turbulence. J. Fluid Mech. 577, 275.

Zaichik, L., Simonin, O., Alipchenkov, V., 2010. Turbulent collision rates of arbitrary-density particles. Int. J. Heat Mass Transfer 53, 1613–1620.

Zaichik, L.I., Alipchenkov, V.M., 2009. Statistical models for predicting pair dispersion and particle clustering in isotropic turbulence and their applications. New J. Phys. 11, 103018.

Zeng, L., Balachandar, S., Najjar, F., 2010. Wake response of a stationary finite-sized particle in a turbulent channel flow. Int. J. Multiphase Flow 36, 403–422.

Zhang, Z., Botto, L., Prosperetti, A., 2006. Microstructural effects in a fully-resolved simulation of 1024 sedimenting spheres. In: Balachandar, S., Prosperetti, A. (Eds.), IUTAM Symposium on Computational Approaches to Multiphase Flow. Springer.

Zhang, Z., Prosperetti, A., 2005. A second-order method for three-dimensional particle simulation. J. Comput. Phys. 210, 292–324.

Zhou, Q., Chang, N., 2009. Experimental investigation of single particle settling in turbulence generated by oscillating grid. Chem. Eng. J. 149, 289–300.

Zimmermann, R., Xu, H., Gasteuil, Y., Bourgoin, M., Volk, R., Pinton, J., Bodenschatz, E., 2010. The Lagrangian exploration module: an apparatus for the study of statistically homogeneous and isotropic turbulence. Rev. Sci. Instrum. 81, 055112.